SECURITY CLASSIFICATION OF THIS PAGE

REPORT DOCUMENTATION PAGE

Form Approved
OMB No. 0704-0188

AD-A245 795

1b RESTRICTIVE MARKINGS

3 DISTRIBUTION/AVAILABILITY OF REPORT
Approved for public release; distribution is unlimited.

4 PERFORMING ORGANIZATION REPORT NUMBER(S)
Technical Report #43

5 MONITORING ORGANIZATION REPORT NUMBER(S)

6a NAME OF PERFORMING ORGANIZATION
Massachusetts Inst. of Tech.

6b OFFICE SYMBOL (If applicable)

7a NAME OF MONITORING ORGANIZATION

6c ADDRESS (City, State, and ZIP Code)
Office of Sponsored Programs
M.I.T., Room E19-702, Cambridge, MA 02139

7b ADDRESS (City, State, and ZIP Code)

8a NAME OF FUNDING/SPONSORING ORGANIZATION
Office of Naval Research

8b OFFICE SYMBOL (If applicable)

9 PROCUREMENT INSTRUMENT IDENTIFICATION NUMBER

8c ADDRESS (City, State, and ZIP Code)
Chemistry Division, Code 1113ES
800 N. Quincy
Arlington, VA 22217-5000

10 SOURCE OF FUNDING NUMBERS

PROGRAM ELEMENT NO	PROJECT NO	TASK NO	WORK UNIT ACCESSION NO
84-K-0553		051-597	

11 TITLE (Include Security Classification)
Well-defined Redox-Active polymers and Block Copolymers Prepared by living Ring-Opening Metathesis Polymerization

12 PERSONAL AUTHOR(S)
D. Albagli, G. Bazan, M.S. Wrighton and R.R. Schrock

13a TYPE OF REPORT	13b TIME COVERED	14 DATE OF REPORT (Year, Month, Day)	15 PAGE COUNT
technical	FROM 90 TO 91	92/2/4	42

16 SUPPLEMENTARY NOTATION
submitted for publication/published in: Journal of the American Chemical Society

17 COSATI CODES			18 SUBJECT TERMS (Continue on reverse if necessary and identify by block number)
FIELD	GROUP	SUB-GROUP	polymers, norbornene derivatives, electrochemistry

19 ABSTRACT (Continue on reverse if necessary and identify by block number)

see attached document.

92-03268

20 DISTRIBUTION/AVAILABILITY OF ABSTRACT	21 ABSTRACT SECURITY CLASSIFICATION	
☐ UNCLASSIFIED/UNLIMITED ☐ SAME AS RPT ☐ DTIC USERS	unclassified	
22a NAME OF RESPONSIBLE INDIVIDUAL Dr. Robert Nowak	22b TELEPHONE (Include Area Code) 202-696-3945	22c OFFICE SYMBOL

DD Form 1473, JUN 86 Previous editions are obsolete SECURITY CLASSIFICATION OF THIS PAGE

S/N 0102-LF-014-6603

Office of Naval Research

Contract N00014-84-K-0553

Task No. 051-597

Technical Report #43

Well -Defined Redox-Active Polymers and Block Copolymers Prepared by living Ring-Opening Metathesis Polymerization

by

D. Albagli, G. Bazan, M.S. Wrighton and R.R. Schrock

Prrepared for Publication

in

the Journal of the American Chemical Society

Massachusetts Institute of Technology
Department of Chemistry
Cambridge, MA 02139

Well-Defined Redox-Active Polymers and Block Copolymers Prepared by Living Ring-Opening Metathesis Polymerization

by

D. Albagli, G. Bazan, M. S. Wrighton,* and R. R. Schrock*

Contribution from

Department of Chemistry
Massachusetts Institute of Technology
Cambridge, Massachusetts 02139

Abstract

Mo(CH-*t*-Bu)(NAr)(O-*t*-Bu)$_2$ (**1a**) in THF/0.1 M [*n*-Bu$_4$N]AsF$_6$ is stable towards reduction out to -2.16 V vs. SCE at a Pt electrode, beyond which it undergoes a reversible, one electron reduction; it is not oxidized at potentials up to 1.0 V. An analogous initiator containing a ferrocenylmethylidene ligand (**1b**) can be synthesized by treating **1a** with vinylferrocene. Redox-active derivatives of norbornene, containing ferrocene (**2**) or phenothiazine (**3**) were prepared and polymerized by **1a** or **1b** to give living block copolymers containing the ring-opened norbornene derivatives. The living polymer was cleaved from the metal in a Wittig-like reaction with pivaldehyde, trimethylsilylbenzaldehyde, or octamethylferrocenecarboxaldehyde. Polydispersities for the longer block copolymers containing up to ~80 monomer units was found to be as low as 1.05 by GPC. In one case the polydispersity of a homopolymer made from the ferrocene-containing monomer was determined by FD-Mass Spectroscopy to be 1.06. DSC studies suggest that microphase formation occurs in the block copolymers, even in the case of relatively low

molecular weight materials. Solution voltammetric studies of homo and block copolymers showed that the redox centers were electrochemically independent, and that all centers exchanged electrons with the electrode. Neutral polymers became insoluble upon oxidation to a polycation, yielding an adsorbed polymer layer on the electrode that could then be cathodically stripped. This oxidative deposition process depended on the electrolyte and the polymer molecular weight, but also could be controlled by the size of a non-electroactive block ir the block copolymers. Problems resulting from precipitation of the redox polymers could be circumvented by employing normal pulse voltammetry. Polymers containing redox-active centers in both end groups, as well as in the polymer chain itself, have been prepared and shown in electrochemical studies to undergo the expected initiation, propagation, and termination reactions.

INTRODUCTION

Studies of electroactive polymers attached to the surface of electrodes have focused more on electrochemical characteristics than on polymer structure. Modification of electrodes with such polymers in order to achieve "molecular electronic" functions, such as pH-dependent charge trapping and chemical sensing[1] has been successful to some degree, but ideally one would like to be able to control the primary structure and the morphology of a polymer to a degree that would maximize the desired electrochemical properties. Such a goal becomes difficult, if not impossible, to achieve using traditional polymer synthesis techniques as the required polymers quickly become relatively exotic and complicated.

The primary structure of an electroactive polymer, and ultimately its morphology (lamellae, rods, or spheres), could be controlled if living polymerization techniques could be employed.[2] Under such circumstances (no chain transfer or termination) the nature of the functionality at each end of the polymer, as well as the nature and length of blocks (containing a given monomer) in the polymer chain could be specified. However, traditional living anionic polymerization methods[3] probably cannot be employed routinely, since relatively sensitive, redox-active groups would be destroyed. Cationic[4] or group transfer methods[5] might be more suitable than anionic methods, but

again some desirable functionalities may not be tolerated. Living ring opening metathesis polymerization (ROMP) of norbornenes and norbornadienes[6,7] appears more promising since functionalized derivatives are relatively easy to synthesize in wide variety by Diels-Alder reactions and since well-characterized ROMP catalysts have been developed that will tolerate many functionalities.[7,8] In this paper we report the synthesis and characterization of electroactive polymers and block copolymers made using living ROMP that demonstrates the potential utility of this approach.

RESULTS AND DISCUSSION

Initiators, Monomers, and Capping Groups.

If polymers are to be prepared from monomers that contain redox active groups the metal catalyst must be electrochemically stable. A cyclic voltammogram of Mo(CH-*t*-Bu)(NAr)(O-*t*-Bu)$_2$ (**1a**) is shown in Figure 1a. The molybdenum complex is not oxidized in THF/0.1M [n-Bu$_4$N]AsF$_6$ at potentials up to 1 V vs. SCE, but it is reduced at -2.16 V at a Pt disk in a one-electron reversible process. A plot of E vs. log[(i_{lim} - i)/i] yields a line of slope RT/nF = 59 mV, with n = 1, indicative of a reversible redox couple.[9] **1a** is electrochemically inactive over a 3V range, and therefore should be stable to reduction or oxidation by most redox active groups that we might choose to incorporate into a monomer.

An initiator that contains a redox-active group can be prepared by adding one equivalent of vinyl-ferrocene to **1a** as shown in eq 1. Polymers prepared with **1b** as the initiator will have one ferrocene as a unique redox active end group. **1b** can be isolated as a bright red crystalline solid in 50-60 % yield. A significant byproduct is [Mo(μ-NAr)(O-*t*-Bu)$_2$]$_2$,[10] which is believed to be the product of coupling of methylene complexes. **1b** itself is relatively stable toward bimolecular

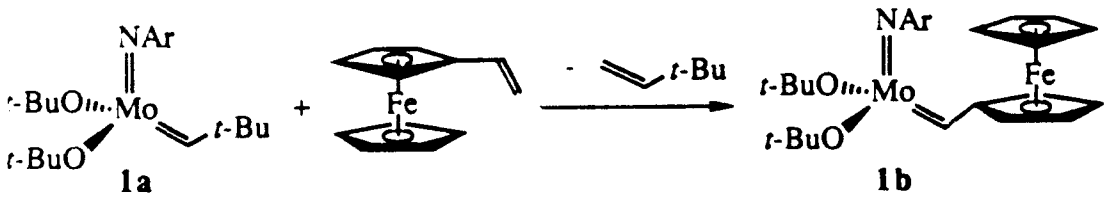

1a **1b** (1)

decomposition. The proton and carbon NMR spectra of **1b** are characteristic of one rotameric form of an alkylidene complex of this general type (δ H_α = 11.90, δ C_α = 274, $J_{CH\alpha}$ = 127), presumably the more stable syn form shown in which the ferrocenyl substituent points toward the imido ligand. Rotamers have been observed in many circumstances[11] and appear to interconvert in systems of this type with $\Delta G^{\ddagger}$ = 16-18 kcal mol^{-1}.

Cyclic voltammograms of **1b** in CH_2Cl_2/0.1 M [*n*-Bu_4N]AsF_6 are shown in Figure 1b. No reduction wave is observed out to -2.40 V vs. SCE, consistent with the ferrocenyl substituent being a stronger electron donor than a *t*-butyl group, thereby making the metal center more difficult to reduce. But *two* overlapping ferrocene-like oxidation waves are observed instead of one. One possible explanation for two waves is the presence of two different conformers with different redox potentials.[12] (Electrochemically-induced structural changes that yield isomers with different redox potentials have been observed for organometallic complexes[13] and hindered olefins.[14]) The rate of interconversion of syn and anti rotamers has been found to be ~1 s^{-1} for similar alkylidene complexes.[11] For **1b** the rate may be slower because of the larger size of the ferrocenyl group. This rate of interconversion should be slow enough so that oxidation of the major rotamer only should be observed. However, if upon oxidation of the ferrocene the rate of rotamer interconversion becomes significantly faster, a situation where two oxidation waves are observed could arise.[15] This possibility is still being evaluated in the case of **1b**. Although decomposition of **1b** has not yet been ruled out completely, different synthetic samples and recrystallized samples all yield the same result, and polymers prepared with **1b** as the initiator produce polymers with the expected stoichiometry (see below).

Initial tests to determine whether a functional group can be tolerated by **1a** consisted of polymerizing norbornene (NBE) in the presence of 30-50 equiv of a molecule containing that functional group. Norbornene polymerization was unaffected by either ferrocene or phenothiazine. In contrast, benzoquinone reacted with **1a** and/or the living polynorbornene and therefore cannot be considered as a potential redox group. Reaction of alkylidene complexes of this type with the carbonyl group in aldehydes and ketones in a Wittig-like reaction is well-known, and the instability

of the alkylidene complexes to benzoquinone therefore is not surprising.

Ferrocene was incorporated into the norbornene skeleton as shown in eq 2. The acid group, which facilitated the Diels-Alder reaction, was later turned into a carbomethoxy group, which is not expected to interfere in polymerization reactions.[7,8] The ferrocenyl and carbomethoxy substituents are trans, but two isomers (presumably endo/exo) were observed. The phenothiazine redox group was introduced as shown in eq 3. This straightforward preparation could be scaled up readily to give gram quantities of trans-2,3-(10'-(2'-ethyl)-phenothiazine)-dicarboxylatonorbornene (**3**) in good yield. The redox potential of **2** was found to be +0.380 V vs. SCE, and that of **3**, which has one redox wave in which two electrons are transferred

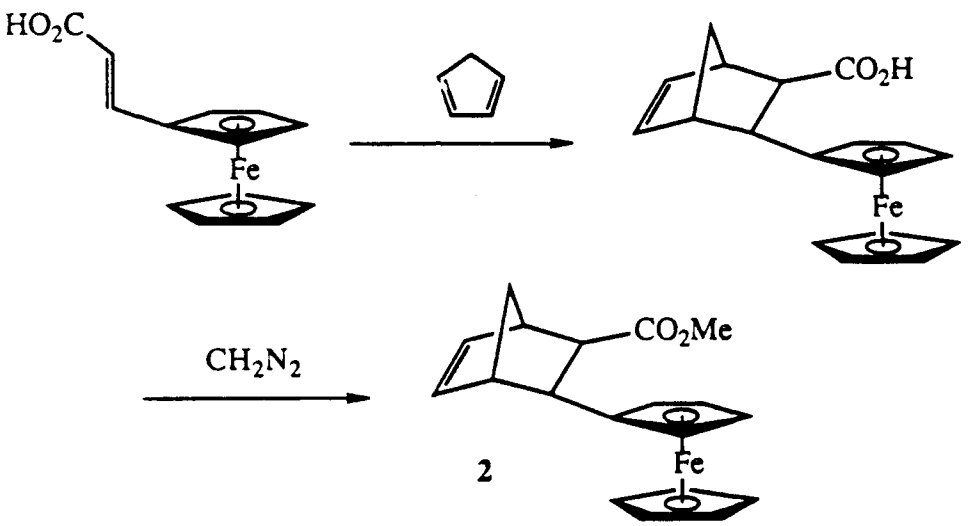

2 (2)

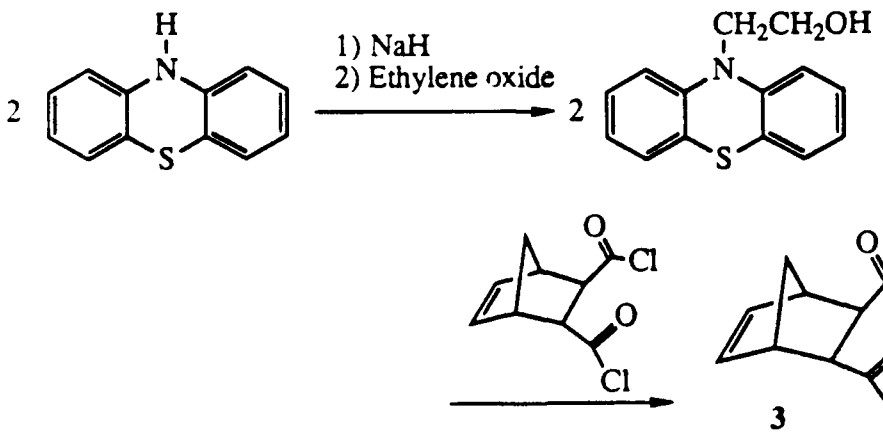

3 (3)

(one from each phenothiazine) was found to be +0.750 V vs. SCE. The ester groups increase the polarity of both **2** and **3**, aiding the solubility of polymers made from them in electrolyte media.

Capping groups can be introduced at the end of a polymerization in a Wittig-like reaction using an aldehyde.[7] In this paper pivaldehyde and trimethylsilylbenzaldehyde have been used as ^{1}H NMR probes for end group analysis, while octamethylferrocenecarboxaldehyde has been employed as a means of introducing a redox-active end group. The polyalkylated ferrocene provides a distinct redox probe, since its redox potential is ~0.8 V negative of the ferrocene unit or units in the monomer or in the initiator. Experiments in which polymers are capped using pyrenecarboxaldehyde, pyridinecarboxaldehyde, and α-bromo-*p*-tolualdehyde will be discussed elsewhere.

Synthesis of Ferrocene-Containing Homopolymers and Block Copolymers

Monomer **2** is polymerized quantitatively employing **1a** as the initiator, and the resulting polymers (after being cleaved from the metal with *p*-trimethylsilylbenzaldehyde) are readily purified by precipitation from non-polar solvents such as hexane, pentane or petroleum ether (Scheme I). GPC analysis shows that the resulting molecular weights are within the narrow range expected for polymers prepared by living systems (Table I). The GPC trace of $(\mathbf{2})_{15}$ (the subscript refers to the average number of monomers per chain) and $(\mathbf{2})_{30}$ each consisted of a single peak with a polydispersity of 1.13, a relatively low value considering the few equivalents of monomer that were employed. ^{1}H and ^{13}C NMR spectra of $(\mathbf{2})_{15}$ and $(\mathbf{2})_{30}$ are broad and complex, as expected for polymers that contain a mixture of cis/trans olefinic linkages, endo/exo, and head to tail isomers.[16] Integration of the TMS group in the cap versus the tert-butyl group in the initiator and the olefinic protons in the backbone yields the result expected from quantitative polymerization and capping in which the most abundant chain has a length equal to the number of equivalents of monomer added. Similar NMR studies of other homopolymers and block copolymers discussed later also were entirely consistent with their formulation. The ratio of the rate constant for propagation versus that for initiation (k_p/k_i) can be measured by NMR techniques under conditions where some, but not all, initiator is consumed, assuming that both initiation and propagation are

first order in catalyst and monomer, and that the rates of the second and subsequent insertion steps are all the same.[17] The k_p/k_i for **2** was found to be ~10, approximately the same (~12) as that found for norbornene.

A more direct measure of the polydispersity in one case was obtained by field desorption mass spectroscopy (FD-MS).[18] Figure 2 shows the doubly charged manifold of peaks obtained for $(\mathbf{2})_{15}$ ranging from n = 8 to n = 26. Singly- and triply-charged peak manifolds were obtained at different values of emitter current. In two manifolds the most abundant chain length was n = 14; it was n = 15 in the third. Employing these data the polydispersity was calculated to be 1.06. This value is in the range of that obtained by GPC, but it may not be totally accurate since the desorbed material may not match the content of the sample. Complete spectra of $(\mathbf{2})_{30}$ could not be obtained by FD-MS.

Block copolymers containing NBE and **2** capped by *t*-butylmethylene (from **1a**) and p-trimethylsilylbenzylidene can be prepared straightforwardly (Table I). Although in these cases norbornene was added first to **1a**, the similarity in the values of k_p/k_i for NBE and **2** suggests that the block copolymers that are formed by adding **2** first would be identical to those obtained by adding NBE first. The polydispersity of these block copolymers are slightly lower than those of the homopolymers, consistent with the longer chain lengths.

Differential scanning calorimetry (DSC) traces of $(\mathbf{2})_n$ homopolymers and $(NBE)_n(\mathbf{2})_m$ block copolymers are shown in Figure 3; glass transition temperatures can be found in Table I. It is evident that the $(NBE)_n$ and $(\mathbf{2})_m$ blocks separate into microphases in the block copolymers, even though the chains are relatively short. For the $(\mathbf{2})_n$ homopolymers, T_g increases with molecular weight, as one would expect, since glass transition temperatures generally do not stop increasing until the molecular weight surpasses ~10,000.[19] In the block copolymers the T_g ascribed to the $(\mathbf{2})_m$ phase is comparatively low (123 and 107°), probably because of the relatively small ratio of domain volume to interphase region for these small blocks. Since the lower T_g block is linked to the higher T_g block, the motion in the polynorbornene block increases the free volume of the $(\mathbf{2})_m$ phase and cooperativity of chain movements is mediated by the chain in the region

between the two phases.[20] As the relative block size of $(NBE)_n$ to $(2)_m$ increases, the magnitude of this effect increases ($T_g(2)$ = 123 °C for $(NBE)_{15}(2)_{15}$ and 107 °C for $(NBE)_{60}(2)_{15}$). Conversely, the lower T_g in block copolymers is higher than that in polynorbornene (~45°C), presumably because the higher T_g domains for $(2)_x$ can dampen chain motions in the region nearby.[2a] As the $(NBE)_n$ block size increases $T_g(NBE)$ is observed at lower temperatures, consistent with the idea that high T_g domains should have less influence as the high T_g monomer becomes a smaller fraction of the polymer composition, i.e., $T_g(NBE)$ = 60 °C for $(NBE)_{15}(2)_{15}$ and 43 °C for $(NBE)_{60}(2)_{15}$.

The electrochemistry of $(2)_n$ and $(NBE)_n(2)_m$ were studied in solution and confined to the electrode surface. The surface-confined electrochemistry will be presented elsewhere. The solution electrochemical behavior of such redox polymers is marked by changes in solubility, which are governed by the amount of charge in the ferrocene units. Reduced (neutral) polymers containing **2** are soluble in benzene, THF, dichloromethane, and dimethylformamide, but insoluble in hexane, ethanol, acetonitrile, and water. In the oxidized state, the polymer is still somewhat soluble in dimethylformamide, but it is insoluble in THF and dichloromethane, and it is only slightly soluble in acetonitrile.

The effects of the solubility properties of $(2)_{15}$ in DMF, THF, and CH_3CN are illustrated in Figure 4. As shown in Figure 4a, in DMF the CV is not much different from that expected for a soluble molecule that has a reversible redox couple, except that the peak cathodic current is ~30% larger than the peak anodic current. In the other solvents the change in solubility with the change in oxidation state is more pronounced. For example, in THF oxidation of $(2)_n$ results in precipitation of the polymer onto the electrode surface, as was also found in electrochemical studies of polyvinyl ferrocene[21] in THF. During the reverse scan, the polymer redissolves as it is reduced. However, adding CH_3CN to the THF electrolyte medium changes the CV of $(2)_{15}$, as shown in Figure 4b. Since the oxidized polymer is slightly soluble in CH_3CN, both neutral and oxidized $(2)_{15}$ are soluble in this mixed solvent; consequently the cathodic stripping peak disappears, and the wave becomes more symmetric

The solubility properties of a redox polymer also depends on polymer composition. Diluting the number of charged sites per chain lowers the charge-to-mass ratio and results in a polymer whose solubility is less affected by the state of charge, as in a block copolymer with a redox active block and a non-redox active block. In Figure 5, the cyclic voltammograms of the polymers containing **2** are shown along with that of ferrocene. The current for the polymer is diminished because of the smaller rate of diffusion. The $(\mathbf{2})_n$ polymers become insoluble in dichloromethane upon oxidation, resulting in a cathodic stripping wave of the adsorbed polymer.[22] The shape of the wave changes with the size of the polymer and percent content of ferrocene.

The hydrodynamic radius of a species determines its diffusion rate.[23] The hydrodynamic radius, sweep rate, and electrode area together determine the nature of the current-voltage curve. The information contained in the relationship among the parameters is expressed by the dimensionless number p[24] (equation 4) where r is a characteristic length of the electrode, v is the sweep rate, D is the diffusion coefficient and the other symbols have their usual meaning. The value of *n* needs to be considered carefully; for these multiredox center polymers n = 1 is appropriate. This point will be discussed later. For $p > 13$ a cyclic voltammogram limited by semi-infinite linear diffusion is obtained, and for $p < 1$ a steady-state curve with radial diffusion is obtained.[24] In the case of ferrocene p = 4.5, so intermediate behavior that approaches the steady-state response is observed, as expected. For polymers, D is much smaller. (Values of D can be estimated from a relation that has been verified by experiment between D and the molecular weight;[23] see the following section.) Estimated values give $p > 15$, so cyclic voltammograms of the polymers are expected to be characterized by linear diffusion with a diffusional tail that decays as $t^{-1/2}$. Instead, the current peaks and then decays to a steady value. This behavior may be attributable to an equilibrium between oxidized polymers precipitated on the electrode and those in the diffusional boundary layer.

$$p = (nF/RT)^{1/2}(r^2v/D)^{1/2} \tag{4}$$

Adding a block of $(NBE)_n$ to $(\mathbf{2})_m$ decreases the amount of material that deposits on the

electrode upon oxidation. For $(NBE)_{60}(\mathbf{2})_{15}$ the ratio of cathodic to anodic peak current is 1 at all sweep rates, notably the slower sweeps (5 to 500 mV s^{-1}). This is the ratio observed for ferrocene, and is the value expected for a reversible couple without adsorption.[9] The $(\mathbf{2})_n$ homopolymers are ~50% by weight ferrocene, whereas $(NBE)_{60}(\mathbf{2})_{15}$, which does not precipitate when oxidized, is 25% by weight ferrocene. In the block copolymers, the charged sites are not evenly distributed along the chain, but are located solely within one block, and thus retain the same local structure as the homopolymers and develop the same charge density in that block when oxidized. However, the solubilizing (non-redox-active) block changes the oxidized block/solvent interaction in a manner that keeps the polymer in solution.

Homopolymers and Block Copolymers that Contain Phenothiazine

A series of homopolymers and block copolymers made from **3** and NBE are shown in Table I. The $(\mathbf{3})_n(NBE)_m$ block polymers were made by adding **3** to **1a** first, followed by NBE. The ratio of k_p/k_i can be determined for **3** as described earlier ; here $k_p/k_i = 5$ for addition of **3** to **1a**. The lower value for k_p/k_i for **3** probably results from the relatively bulky nature of **3**, i.e., the t-butyl group in the initiator is actually sterically smaller than the alkylidene substituent in the growing polymer chain. The polydispersity again decreases as the degree of polymerization increases, as expected. PDI values could not be confirmed by FD-MS for any of these polymers. It should be noted that even the smallest, $(\mathbf{3})_{15}$, is nearly twice the average molecule weight of the polymer that was successfully characterized by FD-MS, $(\mathbf{2})_{15}$. Despite the fact that these polymers have relatively easily ionized redox groups, desorption of the polymer in the electric field must be slower than decomposition.

DSC analyses of polymers containing **3** are shown in Figure 6; glass transition temperatures are listed in Table I. The blocks in $(\mathbf{3})_n(NBE)_m$ also microphase separate. In the block copolymers the main change is the ~10 °C decrease in T_g (**3**) as the length of the $(NBE)_m$ block increases, as found in the case of the $(NBE)_n(\mathbf{2})_m$ polymers discussed earlier. The glass transition of the $(\mathbf{3})_n$ blocks show a distinct endothermic peak, which increases in magnitude the more slowly the sample is cooled through the glass transition region. Slowly annealing the sample

allows it time to approach a lower energy state. Consequently more heat is required to initiate segmental motion, at which point there is an exothermic relaxation to an amorphous state.[25]

The electrochemistry in dichloromethane of a set of $(3)_n$ polymers, $(3)_n(NBE)_m$ block copolymers, and **3** itself was studied in solutions matched in phenothiazine concentration. The sweep rate dependence at moderate rates is shown in Figure 7. The CV of **3** is characteristic of a reversible, Nernstian redox couple with a potential E' = 0.75 V vs. SCE. The CV's of the homopolymers made from **3**, as in the case of homopolymers made from **2**, are marked by a reductive stripping wave due to precipitation of the oxidized material onto the electrode, while the anodic wave maintains the characteristics expected for linear diffusion of the electroactive species. The peak potential is independent of sweep rate and the peak current scales linearly with the square root of the sweep rate up to 500 mV s^{-1}. Note that although **3** contains two equivalents of phenothiazine, there is a single redox wave and the peak separation (ΔE_p = 65 mV) is consistent with a value for n = 1 (59 mV), not n = 2 (29.5 mV). Similarly, cyclic voltammograms of the polymers have only one anodic wave, with no shoulders, and yet contain >20 phenothiazine units. It has been demonstrated for molecules with 2 identical redox sites,[26] and with ~1200 identical redox sites,[27] that reversible oxidation and reduction by 2 or 1200 electrons with a current-potential waveshape characteristic of a one-electron process occurs if the redox sites behave independently of one another. It is the magnitude of the wave that scales with the number of electrons and the diffusion coefficient. Because of oxidative deposition of the $(3)_n$ polymers in dichloromethane , the peak-to-peak separation cannot be used as a criterion of whether the polymers have a one-electron voltammetric waveshape.[9]

Problems with adsorption and precipitation of redox polymers can be overcome by employing normal pulse voltammetry (NPV). In NPV the applied potential is alternatively stepped between the initial potential at the foot of the wave, and a potential that increases with each pulse through the potential region of interest.[28] The duration of each pulse is short (57 ms) in order to minimize precipitation of oxidized material. Since the potential then returns to the initial potential any material that might have deposited is stripped away, and the initial conditions of the experiment

recreated for the next pulse. The current is sampled over the last 17 ms of each potential pulse, i.e., transient currents such as double-layer charging have decayed and the majority of the signal measured is faradaic current. NPV is a form of sampled-current voltammetry, and for reversible couples provides information about the formal potential, the concentration profile, diffusion coefficients and number of electrons in the process.

Normal pulse voltammograms of **3** and $(\mathbf{3})_n$ are shown in Figure 8. Data from the curves, the limiting current, i_{lim}, half-wave potential, $E_{1/2}$, slope of the plot E vs. $\log[(i_{lim} - i)/i]$, and the diffusion coefficient, D_{NPV}, are given in Table II. In the plot of the Heyrovsky-Ilkovic equation (eq 4) the slope is RT/nF and n represents the number of electrons characterizing the waveshape. For n = 1, the slope is 59 mV. The slopes determined for all samples containing **3** agree quite well with this value. Thus the multiple redox sites behave independently, and the polymer passes its electrons in a wave characteristic of a one-electron process. That the polymer passes all of its electrons per redox unit will be shown in the next section using polymers with a redox active end group.

The diffusion coefficient for a randomly coiled, spherical polymer has been shown to be related to the molecular weight[23] as shown in equation 5 for both biological and synthetic materials. This relation can be re-expressed as shown in equation 6 where log(C) arises from the

$$D \alpha MW^{-0.55} \quad (5)$$

$$\log(D) = -0.55\log(MW) + \log(C) \quad (6)$$

proportionality constant in eq 5. A log-log plot of the diffusion coefficient and molecular weight should yield a line with slope -0.55. Values for D calculated in three ways are included in Table II. D_{CV} was determined from the cyclic voltammetric sweep rate dependence. The slope of the plot $i_{p,a}$ vs. $v^{1/2}$ is given by equation 7 where A is the electrode area and C is the concentration of phenothiazine units, and n = 1. D_{SS} was determined from the steady-state current, i_{SS}, in voltammetric sweeps at a 25 mm Pt disk electrode from the relation[29] shown in equation 8 where r

is the electrode radius and the other symbols are defined us usual. D_{NPV} was obtained from the limiting current (i_{lim}) in a normal pulse voltammogram from the simplification of the i-V relation for the limiting current, which is just the Cottrell equation[30] where t is the time at which the current is sampled after a potential pulse.

$$\text{slope} = (2.69 \times 10^5)n^{3/2}ACD^{1/2} \quad (7)$$

$$i_{SS} = 4nFrDC \quad (8)$$

$$i_{lim} = nFAC(D/\pi t)^{1/2} \quad (9)$$

Equation 6 is plotted in Figure 9 for the three sets of diffusion coefficients. The slopes agree well with the theoretical value of -0.55. The data derived from NPV are probably the most reliable. Normal pulse measurements minimize transient currents, since the electrode potential is constant during the measurement. The reproducibility of the measurement manifests itself with each successive pulse in the voltammogram. Because measurements of i_{lim} can be highly accurate, NPV is a good method for determining molecular properties such as diffusion coefficients. With the potential sweep techniques employed here there is the possibility of surface adsorption or precipitation during the sweep, changing the observed current and thus the diffusion coefficient from its true value. The good agreement with the theoretical power relationship, $MW^{-0.55}$ (eq 5), supports the assumption that the polymers assume a randomly coiled spherical conformation in solution.

Polymers Containing Redox-active End Groups

Use of **1b** to initiate polymerizations yields polymers that have a ferrocenylmethylene cap at one end of the chain. Using octamethylferrocenecarboxaldehyde to terminate the reaction yields polymers capped with an octamethylferrocenylmethylene group at the other end. In this way two distinct redox tags can be incorporated. Small polymers were made to more clearly illustrate the redox properties of these materials. The ferrocenylmethylidene complex, **1b**, was found to react more readily than **1a**, i.e., the value of k_p/k_i for polymerization of **3** was found to be 2 for **1b** (versus ~10 for **1a**; see earlier). The results of GPC and DSC analyses are given in Table I. The PDI value is very good considering the relatively short chain length. T_g is lower (by only 7°C)

than the limiting T_g value observed for the larger $(3)_n$ polymers. The presence of one or two ferrocenyl groups should limit the decrease in T_g, since they comprise a significant fraction of the chain.

Cyclic voltammograms of ferrocene-capped polymers of **3** are shown in Figure 10. The redox waves for the end groups have the characteristics of one-electron, reversible, solution couples; the peak potential is independent of scan rate, the peak current is linearly proportional to the square root of the scan rate, and the ratio of peak anodic current to peak cathodic current is roughly one. For Fc-$(3)_5$-$FcMe_8$, a comparison of the peak currents in each wave indicates the ratio of the Fc group in the initiator to the $FcMe_8$ group in the terminating cap is ~1.06. Oxidation and reduction of each does not affect the solubility of the polymer, since solubility is controlled by the larger phenothiazine block. The phenothiazine reduction wave is a spike, indicating that the oxidized material deposits on the electrode. Because of the small size of these polymers precipitation is less pronounced, but it still occurs for polymers that on average consist of five phenothiazine monomer units and have a molecular weight of ~3400. Comparison of the peak currents for the phenothiazine and each of the ferrocene waves yields a ratio of ~12:1; the expected ratio is 10:1. The higher-than expected ratio may not be significant, as the phenothiazine couple is not a simple reversible process because of absorption of the oxidized polymer.

The normal pulse voltammogram of Fc-$(3)_5$-$FcMe_8$ is shown in Figure 11. Values of the limiting currents, half-wave potentials, slopes of the plots E vs. $\log[(i_{lim} - i)/i]$, and diffusion coefficients are given in Table III. The ratio of the components in these redox polymers is more clearly defined in NPV since adsorption and precipitation effects are minimized. At each potential where a pulse is applied the diffusion limited current is proportional to the number of redox sites per polymer that can be oxidized at that potential. At +0.25 V only $FcMe_8$ can be oxidized, at +0.55 V, $FcMe_8$ and Fc can be oxidized, and at +0.90 V, $FcMe_8$, Fc, and **3** are all oxidized. From the diffusion limited currents at these potentials the ratio of the components are determined to be 0.92:1.0:9.6. Similarly, for Fc-$(3)_5$ the ratio determined was 1.0:10.2.

The initiator **1b** provides a unique redox-active end group which is an absolute internal

standard. The NPV results show that the average number of monomer units of **3** in the polymer is equal to the stoichiometry of reagents in the polymerization reaction. Moreover, NPV shows that all redox centers in the polymer exchange electrons with the electrode.

CONCLUSIONS

It has been established that ring opening metathesis polymerization with Mo alkylidene initiators of the type $Mo(CHR')(NAr)(OR)_2$ can be used to make polymers and block polymers that contain redox-active centers with redox potentials between -2.1 V and ~1 V vs. SCE. The primary structure of the polymer (block identity, block size, block order, and end-capping groups) are all controlled as well as is possible in a polymerization process. These redox-active polymers undergo oxidative deposition, but deposition can be moderated by adding non-redox-active blocks to the polymer. On the basis of these studies we expect that these and related molybdenum initiators can be used to produce other well-defined multifunctional polymers, in particular those with blocks containing redox active groups with potentials that increase or decrease uniformly in one direction along the chain.

EXPERIMENTAL

General Procedures. All chemicals used were reagent grade. Tetrahydrofuran was freshly distilled from CaH_2 or Na benzophenone ketyl under dinitrogen immediately prior to use. Pyridine was stored over 4Å molecular sieves. Benzene was stirred with concentrated H_2SO_4, decanted, and distilled under N_2. Anhydrous diethyl ether and the solvents used in chromatography were used as received. 230-400 Mesh silica gel was used in chromatography. N-Nitroso-N-methyl urea, stabilized with 10 wt% CH_3CO_2H, was generously provided by Professor S. Masamune. Ethylene oxide, dicyclopentadiene, pyrrolidine, norbornene, pivaldehyde, ferrocenecarboxaldehyde, *p*-(dimethylamino)benzaldehyde, and 10-methylphenothiazine were obtained from commercial sources. Norbornene was distilled from molten sodium, pivaldehyde was distilled from molecular sieves under dinitrogen, ferrocenecarboxaldehyde, 1-pyrenecarboxaldehyde, and 10-methylphenothiazine were recrystallized from ethanol, and *p*-

(dimethylamino)benzaldehyde was passed through a 5 cm column of activated alumina. Octamethylferrocenecarboxaldehyde,[31] *p*-(trimethylsilyl)benzaldehyde,[32] Mo(CH-*t*-Bu)(NAr)(O-*t*-Bu)$_2$[33] (Ar = 2,6-C_6H_3-*i*-Pr_2), and β-ferrocenylacrylic acid [34] were prepared as described in the literature.

Polymers were synthesized under dinitrogen in a Vacuum Atmospheres drybox. The Mo catalyst (5-10 mg) was dissolved in 1 mL of THF. Monomer was dissolved in THF and the solution was injected into the well-stirred catalyst solution. After an appropriate reaction time, either a second monomer was added, or the living polymer was terminated by adding 3-5 equiv of an aldehyde. When a series of related polymers were made the solution of the living polymer was split at the latest possible point. The polymers were purified by precipitating them twice in hexane, collecting by centrifugation, and drying in vacuo. They were characterized by gel permeation chromatography (GPC) in dichloromethane (0.1-0.3 w/v%) using Shodex KF 802.5, 803, 804, 805, 800P columns, a Knauer differential refractometer, and a Spectroflow 757 absorbance detector.

Differential scanning calorimetry (DSC) and NMR studies were done on commercial instruments. Field desorption mass spectrometry (FD-MS) was done on a JEOL HX110/HX110 instrument by Dr. Catherine Costello.

Electrochemical experiments were done using conventional 3-electrode cells under Ar or N_2. In the case of Mo alkylidene compounds, electrochemical experiments were done in a drybox in cells which had been heated to 110°C under 10^{-6} Torr vacuum. Cyclic voltammetric experiments were performed using a Pine Instruments RDE 4 bipotentiostat modified for low current sensitivity. Normal pulse voltammetry was done using a PAR 174 polarographic analyzer. Traces were recorded on a Kipp and Zonen BD 91 X-Y recorder. The working electrode was a Pt disk made by sealing Pt wire in soft glass. The Pt disk electrodes were polished with 3μ and 1μ diamond paste (Buehler) to a mirror-like finish before use. The counter electrode was a large piece of Pt gauze. The Ag quasi-reference electrode was prepared by dipping a Ag wire in concentrated HNO_3, rinsing with water and methanol and drying. The reference potential was calibrated with

ferrocene (0.380 V vs. SCE, 5 mM in CH_3CN/0.1 M [*n*-Bu_4N]PF_6) and converted to V vs. SCE. [*n*-Bu_4N]AsF_6 was prepared by combining equimolar aqueous solutions of [*n*-Bu_4N]Br and $LiAsF_6$. After 2 h at 4 °C, the solid was collected by filtration and recrystallized from aqueous acetone and water and dried at 110 °C for 48 h, then stored in a dry box. MP 244 °C (Lit[35] 245 °C). [*n*-Bu_4N]PF_6 was recrystallized from 95% ethanol and [*n*-Bu_4N]BF_4 from aqueous acetone.

***trans*-5-Norbornene-3-ferrocenyl-2-carboxylic acid.** The procedure was adapted from the literature.[36] β-Ferrocenylacrylic acid (1.6 g, 6.2 mmol) and *p*-hydroquinone (25 mg, 0.2 mmol) were added under a stream of argon to 25 mL of benzene in a flask fitted with a condenser and gas inlet, glass stoppers and a stir bar. Cyclopentadiene was added to the stirred refluxing solution in 1 mL (15 mmol) portions five times a day over seven days. The progress of the reaction was monitored by proton NMR. The reaction solution was cooled to room temperature, transferred to a separatory funnel and washed three times with 10% $NaHCO_3$. The orange aqueous solution was neutralized with 10% HCl and the resulting precipitate was extracted with diethyl ether until the aqueous phase was colorless. The ether extracts were dried with $MgSO_4$, filtered, and evaporated to give the orange product in 80% and 94% yields (two runs). Two diastereomers were present in a 2:3 ratio in each case: ^{1}H NMR ($CDCl_3$) δ 1.48 (m, 1), 1.66 (m, 0.6), 1.82 (m, 0.4), 2.32 (m, 0.4), 2.75-2.90 (m, 2.2), 3.10 (m, 0.4), 3.23 (m, 0.6), 3.49 (m, 0.4) 4.08 (m, 9), 5.94 (m, 0.4), 6.08 (m, 0.6) 6.26 (m, 0.4), 6.39 (m, 0.6).

***trans*-(exo,endo)-2-Carbomethoxy-(endo,exo)-3-ferrocenyl-5-norbornene (2).** Diazomethane (generated from N-nitroso-N-methyl urea) in diethyl ether was added to a stirred ethereal solution of *trans*-5-norbornene-3-ferrocenyl-2-carboxylic acid. the progress of the reaction was follwed by TLC. The ether was removed by rotary evaporation and the resulting yellow solid was purified by flash chromatography (1:19 ethyl acetate:hexane). The diastereomers were separable by TLC (1:19 ethyl acetate:hexane) and identified on the basis of their ^{1}H and ^{13}C NMR spectra as *exo*-2-carbomethoxy-*endo*-3-ferrocenyl-5-norbornene and *endo*-2-carbomethoxy-*exo*-3-ferrocenyl-5-norbornene. Polymerizations were done using the mixture of diastereomers: ^{1}H NMR of exo, endo mixture (C_6D_6) δ 1.42 (m, 1), 2.01 (m, 1), 2.36 (m, 1), 2.67 (m, 1),

2.91 (m, 1), 3.44 (s, 3), 3.62 (m, 1), 3.71 (m, 1), 3.92 (m, 2), 3.94 (m, 1), 4.06 (s, 5), 5.81 (m, 1), 6.00 (m, 1); endo, exo mixture δ 1.36 (m, 1), 1.51 (m, 1), 2.61 (m, 1), 2.80 (m, 1), 3.05 (m, 1), 3.11 (m, 1), 3.38 (s, 3), 3.96 (m, 4), 4.06 (s, 5), 6.04 (m, 1), 6.26 (m, 1); ^{13}C NMR (C_6D_6) exo, endo mixture δ 43.96, 47.89, 49.04, 49.68, 50.90, 51.52, 66.92, 67.64, 67.74, 68.75, 90.67, 136.22, 136.63, 176.02; endo, exo mixture δ 43.16, 46.42, 47.56, 51.02, 51.21, 51.66, 67.34, 67.83, 67.89, 69.01, 92.15, 133.77, 138.84, 174.36. Anal. Calcd for $C_{19}H_{20}FeO_2$: C, 67.88; H, 6.00; Fe, 16.61; Found: C, 68.34; H, 6.12; Fe, 16.51.

10-(2-Hydroxyethyl)-phenothiazine. Phenothiazine (recrystallized from xylene, 4.95 g, 25 mmol) was dissolved in 20 mL THF and the solution was added to a NaH dispersion (1.0 g of a 60% oil dispersion) in 80 mL THF. The mixture was refluxed for 2 h, cooled to 0 °C, and ethylene oxide (2.4 mL, 50 mmol) was added via cannula. After stirring the mixture for 3 h at 0 °C, it was transferred to a separatory funnel containing saturated aqueous NH_4Cl. The product was extracted with dichloromethane and the extract was washed twice with water, and dried over $MgSO_4$. The mixture was filtered and the filtrate was concentrated by rotary evaporation. Kugelrohr vacuum distillation (168-175 °C/0.15 mm Hg) yielded 5.0 g (83%) of product: ^{1}H NMR ($CDCl_3$) δ 2.00 (m, 1), 3.89 (t, 2), 4.10 (t, 2), 6.89-6.99 (m, 4), 7.14-7.21 (m, 4).

Bis(10-(2-ethyl)-phenothiazine)-*trans*-5-norbornene-2,3-dicarboxylate (3). A 250 mL 3 neck flask was assembled hot with a stopper, gas inlet, septum and stir bar and cooled under Ar. Via cannula, 60 mL THF and then a 20 mL THF solution of 10-(2-hydroxyethyl)-phenothiazine (5.35 g, 22 mmol) and pyridine (1.83 mL, 22 mmol) were added to the flask. *trans*-5-Norbornene-2,3-dicarbonyl chloride (1.56 mL, 10 mmol) was added dropwise via syringe to the stirred solution. After 9 h, the THF was removed by rotary evaporation and the residue taken up in chloroform and water. The phases were separated, the organic phase washed with water, and the aqueous phases extracted the chloroform. The combined organic solutions were dried over $MgSO_4$ and concentrated to a light green, viscous gum. The crude product was chromatographed with a graded elution solvent, from 3:7 to 3:1 ethyl acetate:hexane (EA:Hex). The fractions containing the product were combined and the solvents removed by rotary evaporation. The

resulting white solid was recrystallized from EtOH/$CHCl_3$ to give 3.03 g (48%) of product. R_f (3:7 EA:Hex) 0.39; (1:1 EA:Hex) 0.56; (7:3 EA:Hex) 0.82; MP 121 °C; ^1H NMR ($CDCl_3$) δ 1.33 (m, 1), 1.44 (m, 1), 2.64 (m, 1), 3.04 (m, 1), 3.17 (m, 1), 3.32 (m, 1), 4.07 (t, 2), 4.14 (t, 2), 4.33 (t, 2), 4.41 (t, 2), 5.85 (m, 1), 6.14 (m, 1), 6.90 (m, 8), 7.12 (m, 8); ^{13}C NMR ($CDCl_3$) δ 45.8, 46.0, 47.1, 47.4, 47.6, 47.9, 61.0, 61.3, 115.3, 115.4, 122.9, 125.3, 125.4, 127.4, 127.6, 135.0, 137.6, 144.7, 173.2, 174.3. Anal. Calcd for $C_{37}H_{32}N_2O_4S_2$: C, 70.23; H, 5.10; N, 4.43; S, 10.13; Found: C, 70.22; H, 5.12; N, 4.42; S, 10.24.

Mo(CHFc))(NAr)(O-*t*-Bu)$_2$ (1b; Fc = Ferrocenyl). Vinyl ferrocene (65 mg, 0.31 mmol) and **1a** (150 mg, 0.31 mmol) were placed together as solids and the minimum amount of toluene (~1-2 mL) needed to dissolve the two was added. The solution color changed from dark orange to bright red as a light red solid precipitated out of solution. The mixture was stirred for 48 hours after which the solvents were removed *in vacuo*. The red residue was extracted with pentane (1-2 mL) and the extracts filtered through Celite. Recrystallization from a minimum amount of pentane at -40 °C gave the product as bright red needles in two crops (82 mg, 43 %): ^1H NMR δ 11.90 (s, 1, $H\alpha$), 7.05 (m, 3, Ar-N-2,6-$C_6H_3(CHMe_2)_2$), 4.21 (dd, 2, $C\alpha C_5H_4Fe$), 4.09 (s, 5, C_5H_5Fe), 4.00 (sept, 2, N-2,6-$C_6H_3(CHMe_2)_2$), 3.97 (dd, 2, $C\alpha C_5H_4Fe$), 1.35 (s, 18, $OCMe_3$), 1.08 (d, 12, N-2,6-$C_6H_3(CHMe_2)_2$); ^{13}C NMR δ 2.74 ($C\alpha$, J_{CH} = 127), 155.5 (C_{ipso}), 146.3 (C_o), 127.2 (C_p), 123.1 (C_m), 95.1 ($C\beta$), 77.2 ($OCMe_3$), 69.3 ($C\alpha C\beta(CH_2)_4Fe$), 69.3 (C_5H_5Fe), 68.2 (($C\alpha C\beta(CH_2)_4Fe$), 32.0 ($OCMe_3$), 28.4 ($CHMe_2$), 27.8 ($CHMe_2$). Anal. Calcd for $MoC_{31}H_{45}FeNO_2$: C, 60.50; H, 7.37; N, 2.28. Found: C, 60.28; H, 7.44; N, 2.07.

Preparation of Polymers. Representative preparations of several polymers are described here. Other preparations were analogous. The extent of conversion of capping reactions with the various aldehydes was followed by monitoring the loss of the alkylidene proton resonance at ~11.6 ppm. See Table I for characterization data.

(2)$_{15}$. A solution of **2** (103 mg, 3.1×10^{-4} mol) in THF (1 mL) was added quickly to a rapidly stirred solution of **1a** (10 mg, 2.05×10^{-5} mol) in THF (1.0 mL). After 15-20 minutes the reaction was quenched with an excess of pivaldehyde (20 μL). After 30 minutes the polymer

was precipitated by pouring the reaction mixture into 200 mL of hexane, was isolated by centrifugation, and was dried in vacuo for several hours; yield 95 mg (92%) of a light orange powder. The ^{1}H NMR spectrum shows an olefinic proton resonance for trans double bonds in the backbone at ~4.1 ppm and a cis olefinic proton resonance at ~3.7 ppm in a ratio of approximately 2:1. ^{13}C NMR ($CDCl_3$) δ 174.6, 175.0, 129-134 (olefinic region), 91.8, 89.9, 70, 68.4, 67.2, 66.7, 65.1, 55.1, 51.8, 51.4, 47.5, 45.5, 41, 39, 29.8.

$(3)_{15}$. A solution of **3** (128 mg, 3.05 × 10^{-4} mol) in THF (1 mL) was added quickly to a rapidly stirred solution of **1a** (10 mg, 2.05 × 10^{-5} mol) in THF (1 mL). After 15 minutes the reaction was quenched with an excess of pivaldehyde (20μL) and the polymer was isolated as described above as a cream-colored powder (120 mg, 94%): ^{1}H NMR ($CDCl_3$) δ 7.02 (b, 8), 6.78 (b, 8), 5.19 (b, 2), 4.22 (b, 4), 3.93 (b, 4), 3.2-2.4 (b, 4), 1.66 (b, 1), 1.34 (b, 1), 0.94 and 0.91 and 0.89 (s, 0.9); ^{13}C NMR ($CDCl_3$) δ 173.2, 172.5, 144.5, 133.5, 132.3, 130.8, 129.9, 127.6, 125, 123, 115, 60.5, 52.3, 51.2, 46, 44.5, 39.0, 32.6, 29.5.

$(NBE)_{60}(2)_{15}$. A solution of norbornene (115.8 mg, 1.23 x 10^{-3} mol) in THF (1.0 mL) was added quickly to a well-stirred solution of **1a** (10 mg, 2.05 x 10^{-5} mol) in THF (1.0 mL). After 5 min a solution of **2** (103.4 mg, 3.08 x 10^{-4} mol) in THF (1 mL) was added quickly to the reaction. After 10 min *p*-trimethylsilylbenzaldehyde (20 μL, 1.1 x 10^{-4} mol) was added. After 10 min the reaction mixture was added slowly to 100 mL of stirred hexane and the light yellow precipitate was collected by centrifugation, reprecipitated in hexane, and dried under vacuum to give 195 mg (90%) of the product as a yellow powder. Proton and carbon NMR spectra were a superposition of those for the homopolymers in the expected ratio. The ratio of trimethylsilyl to t-butyl end groups was 1:1.

Fc-$(3)_5$-$FcMe_8$. **3** (127 mg, 2.0 × 10^{-4} mol) was dissolved in 900 μL of C_6D_6 and added quickly to a solution of **1b** (25 mg, 4.1 × 10^{-5} mol) in C_6D_6 (900 μL). After 15-20 minutes the resulting solution was split into 3 × 600 μL portions, the first was immediately quenched by addition of 15 μL of pivaldehyde and served as a standard for the polymerization of **3**. Octamethylferrocenecarboxaldehyde (11 mg, 3.3 × 10^{-5} mol) in C_6D_6 (100 μL) was added to

another portion. To the last portion a solution of 2-triethoxysilyl-5-norbornene (7 mg, 2.7×10^{-5} mol, 2 equivalents relative to concentration of propagating alkylidene) in C_6D_6 (200 μL) was added under vigorous stirring, stirred for an additional 10 minutes and finally quenched with octamethylferrocenecarboxaldehyde (11 mg, 3.3×10^{-5} mol) in C_6D_6 (100 μL). The oligomers were purified in the usual fashion.

Acknowledgements

R.R.S. thanks the National Science Foundation (DMR 87-19217) and Nippon-Zeon for support. G.B. thanks NSERCC for a postdoctoral fellowship. M.S.W. thanks the Office of Naval Research and the Defense Advanced Research Projects Agency for partial support of this research.

References

1. (a) Smith, D. K.; Tender, L. M.; Lane, G. A.; Licht, S.; Wrighton, M. S. *J. Am. Chem. Soc.* **1989**, *111*, 1099. (b) Shu, C-F.; Wrighton, M. S. *J. Phys. Chem.* **1988**, *92*, 5221.

2. (a) Odian, G. *Principles of Polymerization;* Wiley: New York, NY, 1981. (b) Rempp, P.; Merrill, E. *Polymer Synthesis;* Huethig & Wepf: Heidelberg, 1986. (c) Gold, L. *J. Chem. Phys.* **1958**, *28*, 91. (d) Flory, P. *J. Am. Chem. Soc.* **1940**, *62*, 1561. (e) Szwarc, M. *Nature* **1956**, *178*, 1168.

3. Szwarc, M. *Carbanions, Living Polymers, and Electron Transfer Processes*; Wiley: New York, 1968.

4. Miyamoto, M.; Sawamoto, M.; Higashimura, T. *Macromolecules* **1984**, *17*, 265.

5. Sogah, D. Y.; Webster, O. W. *Macromolecules* **1986**, *19*, 1775.

6. Grubbs, R. H.; Tumas, W. *Science* **1989**, *243*, 907.

7. Schrock, R. R. *Acc. Chem. Res.* **1990**, *24*, 158.

8. (a) Bazan, G. C.; Schrock, R. R.; Cho, H.-N. *Macromolecules*, in press. (b) Bazan, G. C.; Oskam, J. H.; Cho, H.-N.; Park, L. Y.; Schrock, R. R. *J. Am. Chem. Soc.*, in press.

9. Bard, A. J.; Faulkner, L. R. *Electrochemical Methods*; Wiley: New York, 1980, Chapter 5.

10. Robbins, J.; Schrock, R. R. *Organometallics*, in press.

11. Schrock, R. R.; Crowe, W. E.; Bazan, G. C.; DiMare, M.; O'Regan, M. B.; Schofield, M. H. *Organometallics*, in press.

12. Evans, D. H.; O'Connell, K. M. *Electroanalytical Chem.* **1986**, *14*, 113.

13. Wimmer, F. L.; Snow, M. R.; Bond, A. M. *Inorg. Chem.* **1986**, *14*, 113.

14. Evans, D. H.; Busch, R. W.; *J. Am. Chem. Soc.* **1982**, *104*, 5057.

15. Bond, A. M.; Oldham, K. B. *J. Phys. Chem.* **1983**, *87*, 2492.

16. Ivin, K. J. *Olefin Metathesis*; Academic Press: London; 1983.

17. Bazan, G.; Khosravi, E.; Schrock, R. R.; Feast, W. J.; Gibson, V. C.; O'Regan, M. B.; Thomas, J. K.; Davis, W. M. *J. Am. Chem. Soc.* **1990**, *112* , 8378.

18. (a) Saito, J.; Waki, H.; Teramae, N.; Tanaka, S. *Prog. Org. Coatings* **1988**, *15*, 311. (b) Lattimer, R. P.; Schutten, H-R. *Anal. Chem.* **1989**, *61*, 1201A.

19. Elias, H.-G. *Macromolecules*; Plenum: New York, 1984; Chapter 10.

20. Morèse-Séquéla, B.; St.-Jacques, M.; Renaud, J. M.; Prud'homme, J. *Macromolecules*, **1980**, *13*, 100.

21. Flanagan, J. B.; Margel, S.; Bard, A. J.; Anson, F. C. *J. Am. Chem. Soc.* **1978**, 100, 4248.

22. (a) Merz, A.; Bard, A. J. *J. Am. Chem. Soc.* **1978**, *100*, 3222. (b) Smith, T. W.; Kuder, J. E.; Wychik, D. J. *J. Polym. Sci.* **1976**, *14*, 2433.

23. Tanford, C. *The Physical Chemistry of Macromolecules*; Wiley: New York, 1961.

24. Aoki, K.; Akimoto, K.; Tokuda, K.; Matsuda, H.; Osteryoung, J. *J. Electroanal. Chem.* **1984**, 171, 219.

25. Burfield, D. R.; Lim, K.-L. *Macromolecules* **1983**, *16*, 1170.

26. Ammar, F.; Savéant, J. M. *J. Electroanal. Chem.* **1973**, *47*, 115.

27. Saji, T.; Paseh, N. F.; Webber, S. E.; Bard, A. J. *J. Phys. Chem.* **1978**, *82*, 1101.

28. (a) Parry, E. P.; Osteryoung, R. A. *Anal. Chem.* **1965**, *37*, 1635. (b) Osteryoung, J. G.; Schreiner, M. M. *CRC Crit. Rev. Anal. Chem.* **1988**, *19*, S1.

29. Saito, Y. *Rev. Polarogr.* **1968**, *15*, 178.

30. Delahay, P. *New Instrumental Methods in Electrochemistry*; Interscience Publishers: New York, NY, 1954, p. 57.

31. Zou, C.-F.; Wrighton, M. S. *J. Am. Chem. Soc.* **1990**, *21*, 7578.

32. Wilbur, D. S.; Svita, Z. V. *J. Label. Compds. Radiopharm.* **1984**, *21*, 415.

33. Schrock, R. R.; Murdzek, J. S.; Bazan, G. C.; Robbins, J.; DiMare, M.; O'Regan, M. *J. Am. Chem. Soc.* **1990**, *112*, 3875.

34. Osgerby, J. M.; Pauson, P. L. *J. Chem. Soc.* **1958**, 650.

35. Compton, S.; Wang, H. H.; Williams, J. M. *Inorg. Syn.* **1986**, *24*, 138.

36. Nicolas, L.; Beugelmans-Verrier, M.; Guilhem, J. *Tetrahedron* **1981**, *37*, 3847.

Table I. Characterization of Redox-Active Polymers and Block Copolymers

Polymer[a]	PDI[b]	M_n[c]	MW(calc)	T_g[d]
$(\mathbf{2})_{15}$	1.13	5090	5250	143
$(\mathbf{2})_{30}$	1.13	9030	10290	150
$(NBE)_{15}(\mathbf{2})_{15}$	1.05	10460	6688	60, 123
$(NBE)_{60}(\mathbf{2})_{15}$	1.07	16190	10930	43, 107
$(\mathbf{3})_{15}$	1.20	8360	9630	88
$(\mathbf{3})_{30}$[e]	1.10	14750	19190	88
$(\mathbf{3})_{30}(NBE)_{50}$	1.12	26740	23830	45, 91
$(\mathbf{3})_{10}(NBE)_{70}$	1.08	35860	13060	50, 80
Fc-$(\mathbf{3})_5$ or Fc-$(\mathbf{3})_5$-$FcMe_8$[f]	1.22	2700	3430	81

[a]Polymer end groups are those shown in Scheme I unless otherwise noted. [b]Polydispersity index determined by gel permeation chromatography. For $(\mathbf{2})_{15}$ the PDI measured by FD-MS (see text and Figure 2) was 1.06. [c]M_n determined by GPC vs. polystyrene. [d]Determined by DSC (scan rate 20 °C/min). [e]The end cap is p-(N,N-dimethylamino)phenylmethylene. [f]Fc = ferrocenylmethylene; $FeMe_8$ = octamethylferrocenylmethylene; Fc-$(\mathbf{3})_5$ was capped with pivaldehyde.

Table II. Data From Normal Pulse Voltammetric Oxidation.

Species	i_{lim}[a]	$E_{1/2}$[b]	slope[c]	D_{npv}[d]	D_{ss}[e]	D_{cv}[f]
3	0.44	750	-61	9.4	11.0	25.0
$(3)_{15}$	0.21	740	-62	2.6	3.4	12.0
$(3)_{30}(NBE)_{50}$	0.16	740	-58	1.3	2.1	4.4
$(3)_{10}(NBE)_{70}$	0.19	750	-61	1.9	2.8	4.6

[a] mA [b] mV vs. SCE. [c] Slope of the plot E vs. $\log[(i_{lim} - i)/i]$ in mV. [d] Calculated from eq 6 in units of $cm^2\ s^{-1} \times 10^6$. [e] Calculated from eq 4. [f] Calculated from eq 3.

Table III. Data From Normal Pulse Voltammetric Oxidation of Polymers With Redox-Active End Groups

		Fc-(3)$_5$			Fc-(3)$_5$-FcMe$_8$	
Component	i_{lim}(nA)	$E_{1/2}$(mV)[a]	slope(mV)[b]	i_{lim}	$E_{1/2}$	slope
FcMe$_8$				9.5	5	-72
Fc	12	410	-70	10.3	380	-86
Phenothiazine	122	750	-56	101.2	750	-58
Diff. Coef. (cm^2 s^{-1})						
D_{obs}[c]		6.7×10^{-6}			5.2×10^{-6}	
D_{calc}[d]		4.8×10^{-6}			4.7×10^{-6}	

[a]vs. SCE. [b]slope of the plot E vs. $\log[(i_{lim} - i)/i]$. [c]Calculated from eq 6 using i_{lim} from Fc wave. [d]Calculated from the relation $D_i = D_j(MW_j/MW_i)^{0.55}$ using ferrocene for the comparison; MW = 186, D = 2.4×10^{-5} (Kadish, K. M.; Ding, J. Q.; Malinski, T. *Anal. Chem.* **1984**, *56*, 1741).

Figure Captions

Figure 1. Cyclic voltammetry of (a) **1a** in THF/0.1 M [*n*-Bu_4N]AsF_6 at 25 mV s^{-1} at a 25 μm Pt disk electrode and (b) **1b** in CH_2Cl_2/0.1 M [*n*-Bu_4N]AsF_6 at 50 and 500 mV s^{-1} at a 500 μm Pt disk electrode.

Figure 2. The doubly-charged manifold of peaks in the field desorption mass spectrum of $(2)_{15}$.

Figure 3. DSC traces of the $(2)_n$ polymers and $(NBE)_m(2)_n$ block copolymers. (Scan rate 20 °C/min.) Samples were annealed above the transition temperature for 10 min, and all measurements were repeated.

Figure 4. Solvent dependence of the cyclic voltammograms of $(2)_{15}$. (a) DMF/0.1 M [*n*-Bu_4N]BF_4; (b) THF, 1:1 THF:CH_3CN, and 1:6 THF:CH_3CN. (The supporting electrolyte was 0.1 M [*n*-Bu_4N]BF_4).

Figure 5. Comparison of the cyclic voltammograms of ferrocene, $(2)_{15}$, $(2)_{30}$, $(2)_{15}(NBE)_{15}$, and $(2)_{15}(NBE)_{60}$ in CH_2Cl_2/0.1 M [*n*-Bu_4N]PF_6. The concentration of ferrocene centers is the same (3.0 mM) in each case.

Figure 6. DSC traces of the $(3)_n$ polymers and $(3)_n(NBE)_m$ block copolymers. (Scan rate was 20 °C/min.) The samples were first annealed above the transition temperature for 10 min, and all measurements were repeated.

Figure 7. Scan rate dependence of the **3**, $(3)_{15}$, $(3)_{30}(NBE)_{50}$, and $(3)_{10}(NBE)_{70}$ in CH_2Cl_2/0.1 M [*n*-Bu_4N]PF_6. The concentration of phenothiazine centers is the same for all solutions (0.2 mM).

Figure 8. Normal pulse voltammograms of **3**, $(3)_{15}$, $(3)_{30}(NBE)_{50}$, and $(3)_{10}(NBE)_{70}$ in CH_2Cl_2/0.1 M [*n*-Bu_4N]PF_6. The current was sampled over the last 17 ms of a 57 ms pulse. (Sweep rate 10 mV s^{-1}; drop time 1 s.)

Figure 9. Log-log plot of the diffusion coefficient vs. the molecular weight of a series of phenothiazine polymers, and a least-squares fit of the data. The diffusion coefficients were obtained experimentally by cyclic voltammetry, steady-state cyclic voltammetry, and normal pulse voltammetry.

Figure 10. Cyclic voltammograms of Fc-(**3**)$_5$ and Fc-(**3**)$_5$-FcMe$_8$ in CH_2Cl_2/0.1 M [*n*-Bu_4N]AsF_6 at a 500 μm Pt disk electrode. In the first cycle the potential sweep was reversed at +0.50 V; in the second cycle it was reversed at +1.00 V.

Figure 11. Normal pulse voltammogram of Fc-(**3**)$_5$-FcMe$_8$ in CH_2Cl_2/0.1 M [*n*-Bu_4N]PF_6. The current was sampled for the last 17 ms of a 57 ms pulse. (Sweep rate 10 mV s^{-1}; drop time 1 s.)

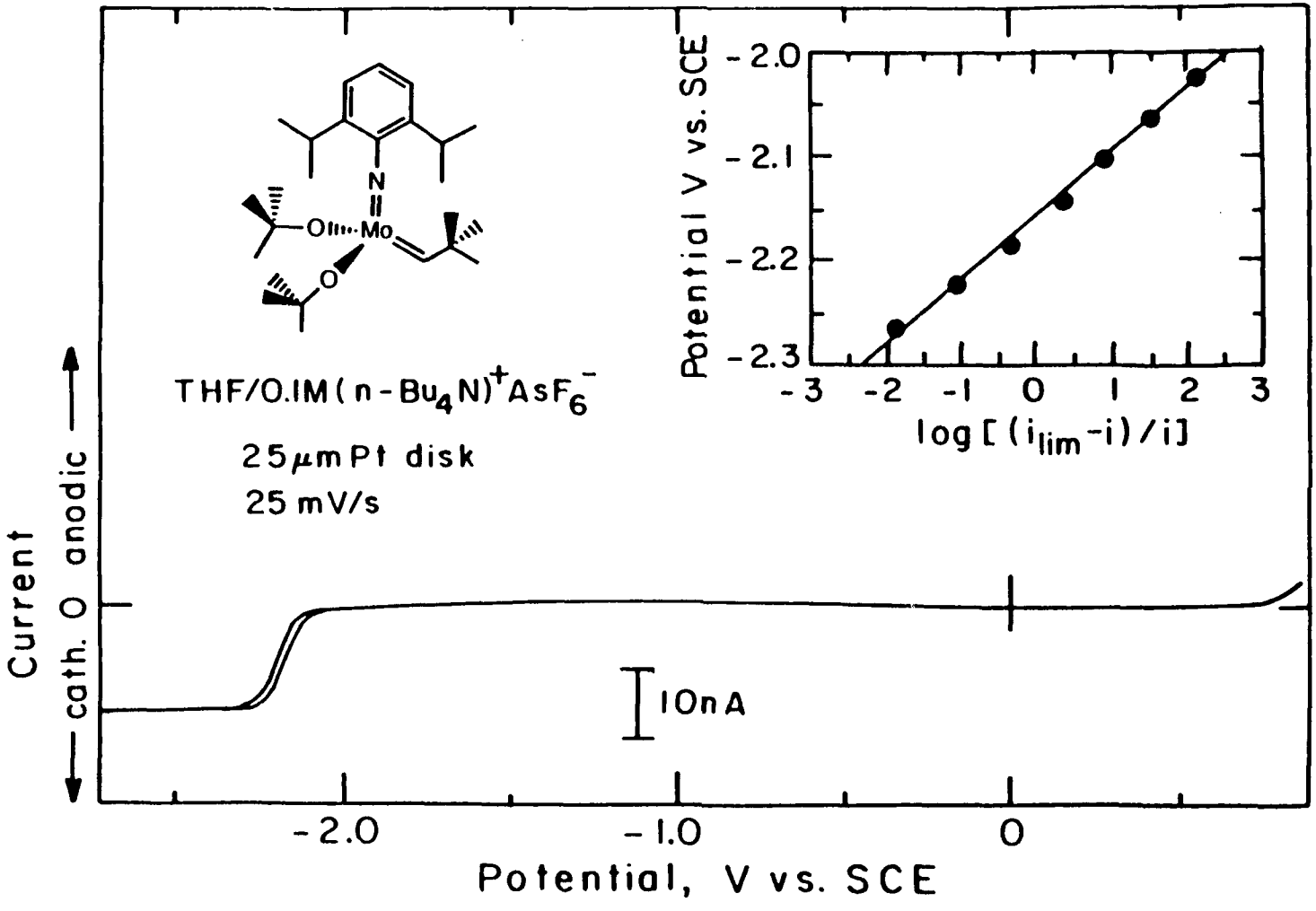
THF/0.1M(n-Bu4N)+AsF6-
25μm Pt disk
25 mV/s
Current
cath. O anodic
10nA
-2.0
-1.0
0
Potential, V vs. SCE
Potential V vs. SCE
-2.0
-2.1
-2.2
-2.3
-3
-2
-1
0
1
2
3
log [(ilim-i)/i]

Fig 1a

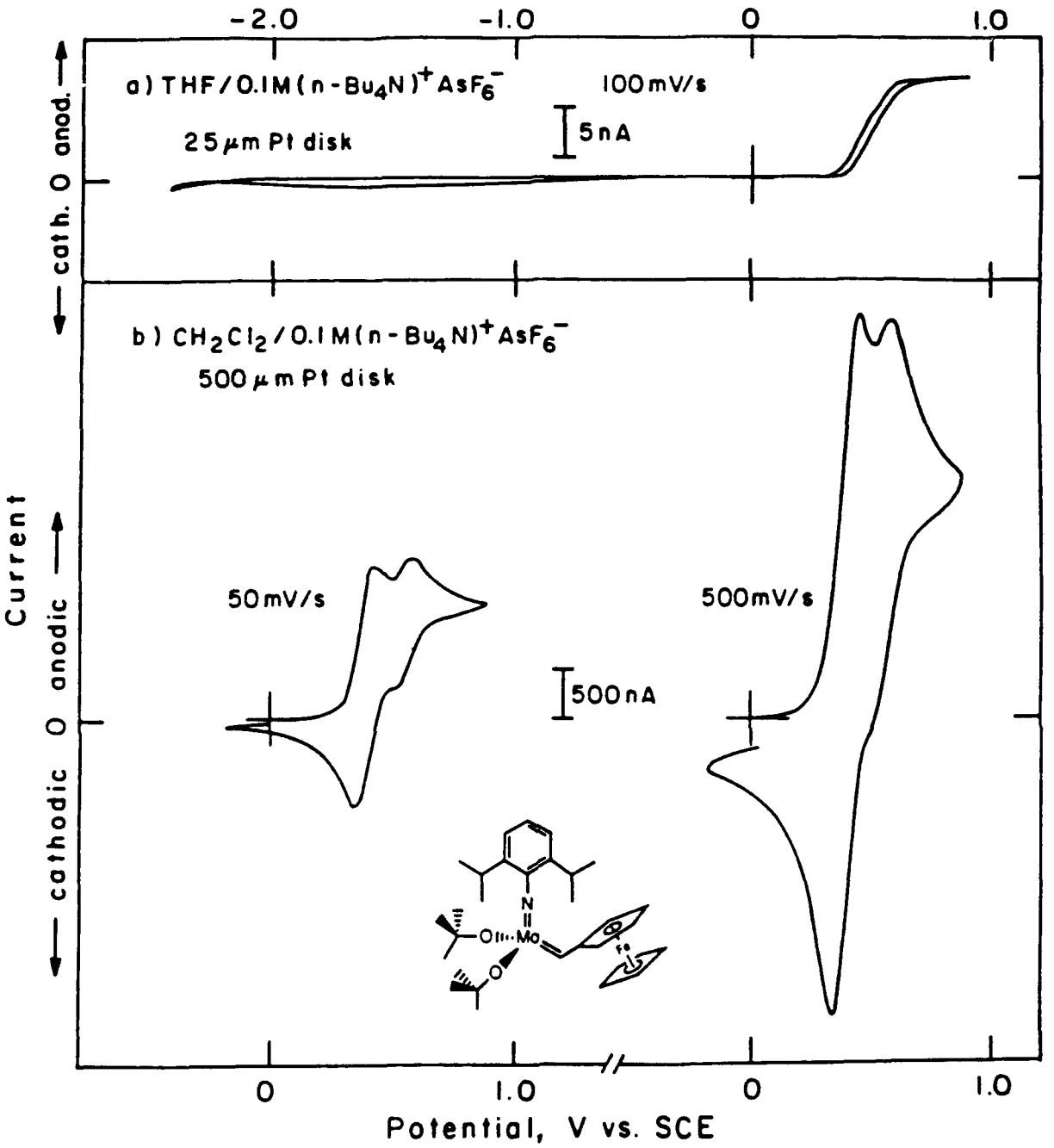
-2.0
-1.0
0
1.0
a) THF/0.1M(n-Bu4N)+AsF6-
100mV/s
25μm Pt disk
5nA
cath. 0 anod.
b) CH2Cl2/0.1M(n-Bu4N)+AsF6-
500μm Pt disk
Current
50mV/s
500mV/s
500nA
cathodic 0 anodic
N
O
Mo
0
1.0
0
1.0
Potential, V vs. SCE

Fig. 1c

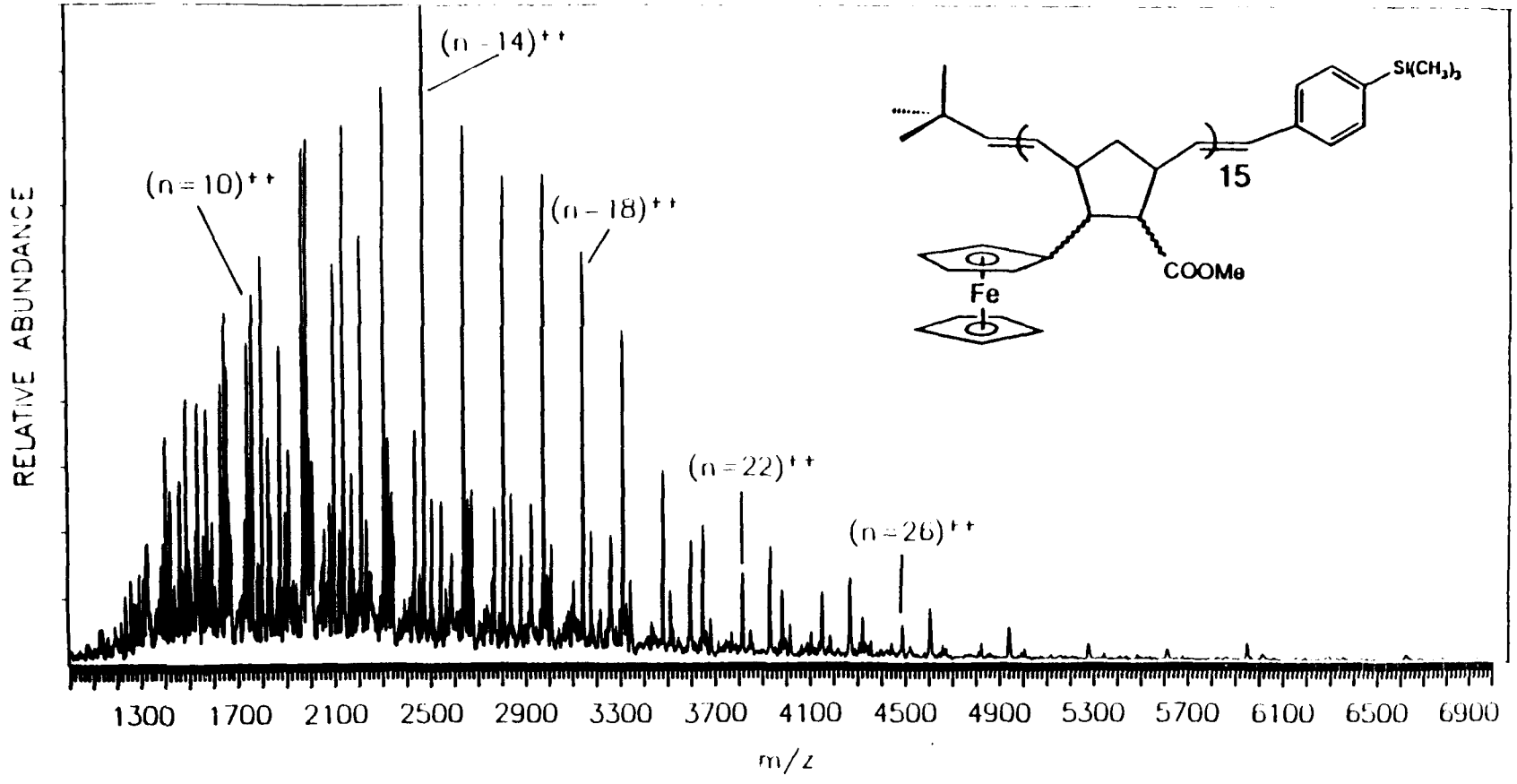
(n = 14)++
(n = 10)++
(n = 18)++
(n = 22)++
(n = 26)++
RELATIVE ABUNDANCE
1300 1700 2100 2500 2900 3300 3700 4100 4500 4900 5300 5700 6100 6500 6900
m/z
Si(CH3)3
15
COOMe
Fe

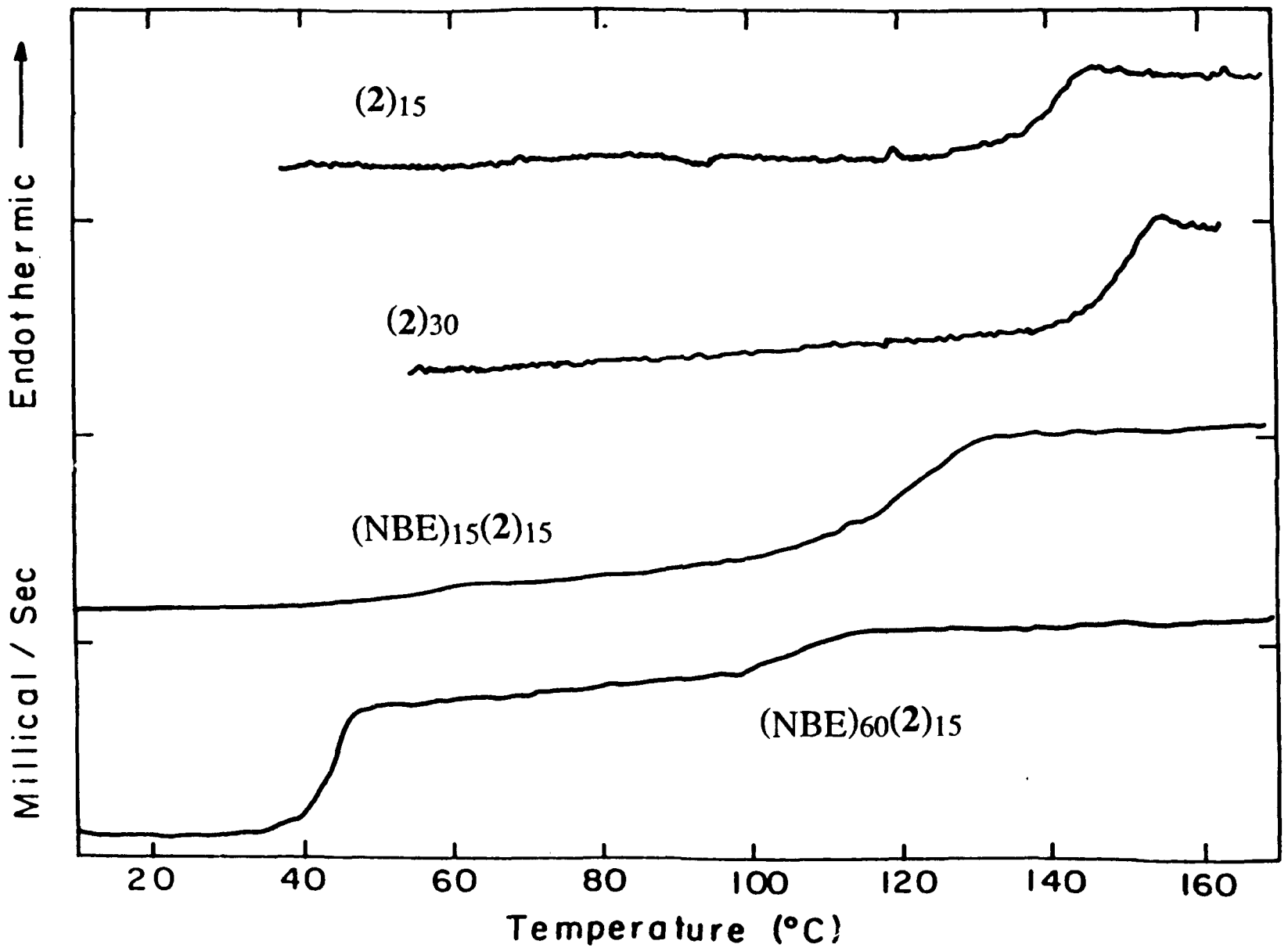
(2)15
(2)30
(NBE)15(2)15
(NBE)60(2)15
Endothermic
Millical / Sec
20
40
60
80
100
120
140
160
Temperature (°C)

Fig 3

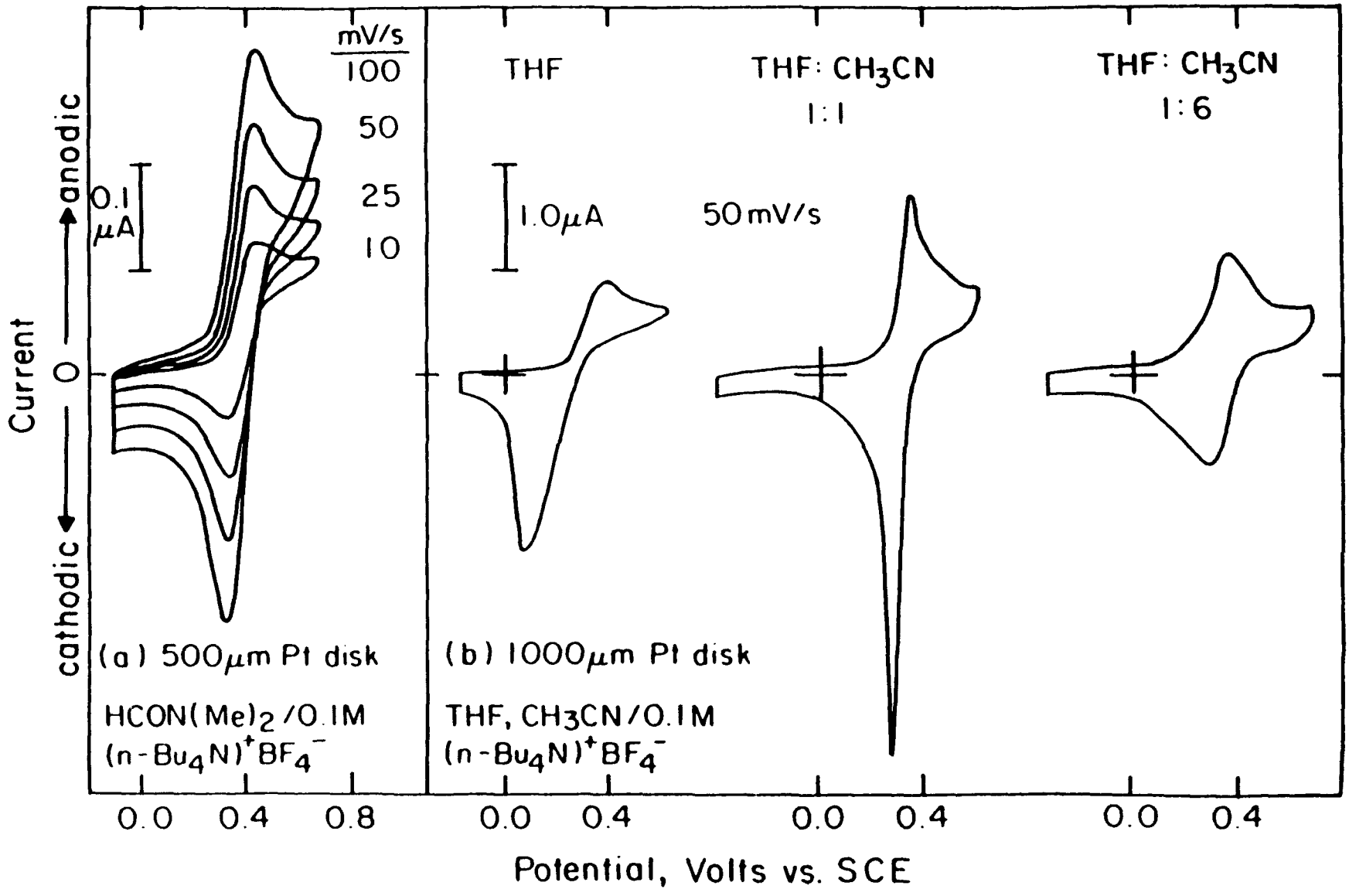
mV/s
100
50
25
10
0.1 μA
1.0μA
50 mV/s
THF
THF: CH3CN
1:1
THF: CH3CN
1:6
Current
anodic
0
cathodic
(a) 500μm Pt disk
HCON(Me)2 /0.1M
(n-Bu4N)+BF4−
(b) 1000μm Pt disk
THF, CH3CN/0.1M
(n-Bu4N)+BF4−
0.0
0.4
0.8
0.0
0.4
0.0
0.4
0.0
0.4
Potential, Volts vs. SCE

Fig 4

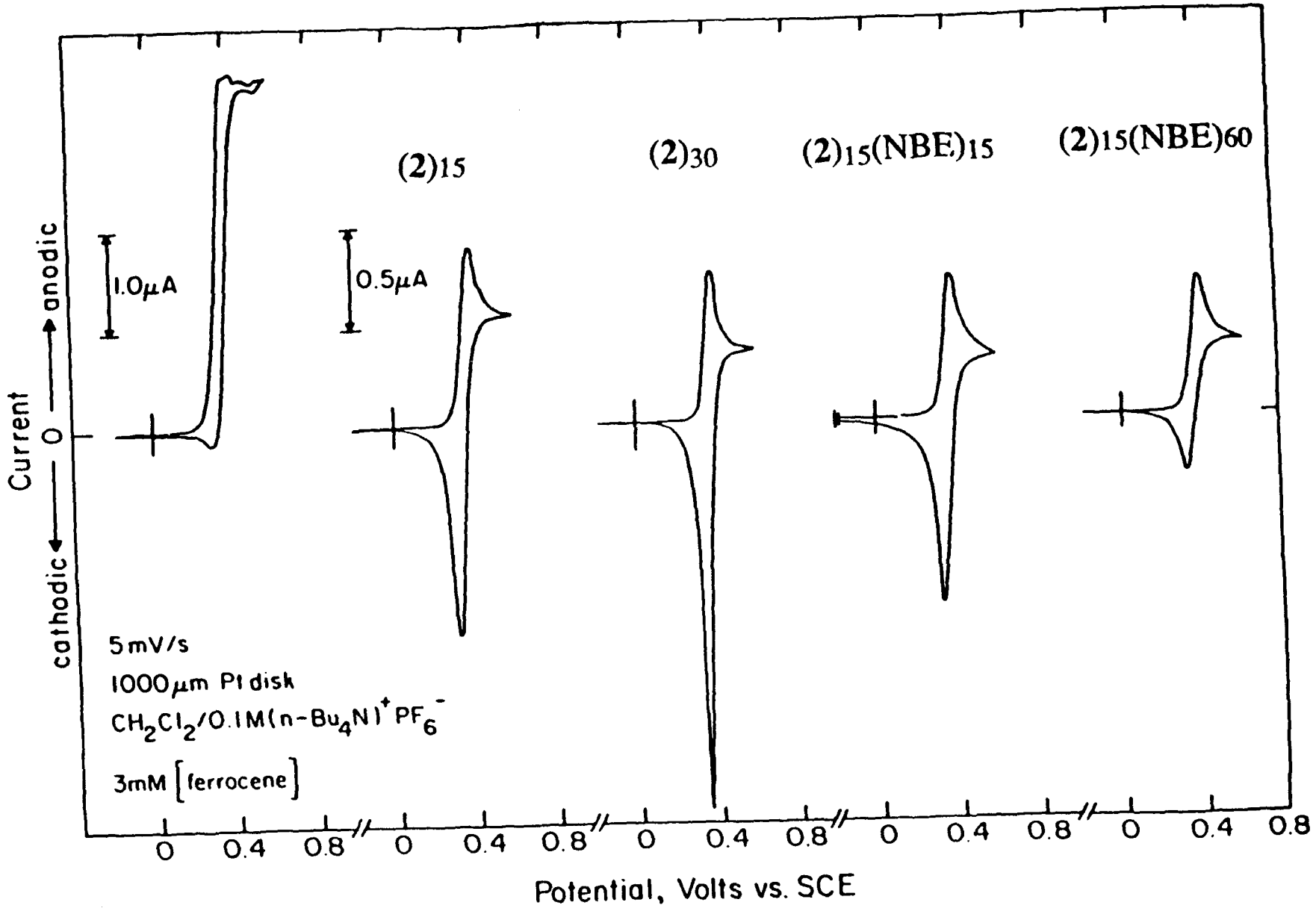
(2)15
(2)30
(2)15(NBE)15
(2)15(NBE)60
1.0μA
0.5μA
Current
anodic
0
cathodic
5mV/s
1000μm Pt disk
CH2Cl2/0.1M(n-Bu4N)+PF6-
3mM [ferrocene]
0
0.4
0.8
Potential, Volts vs. SCE

Fig 5

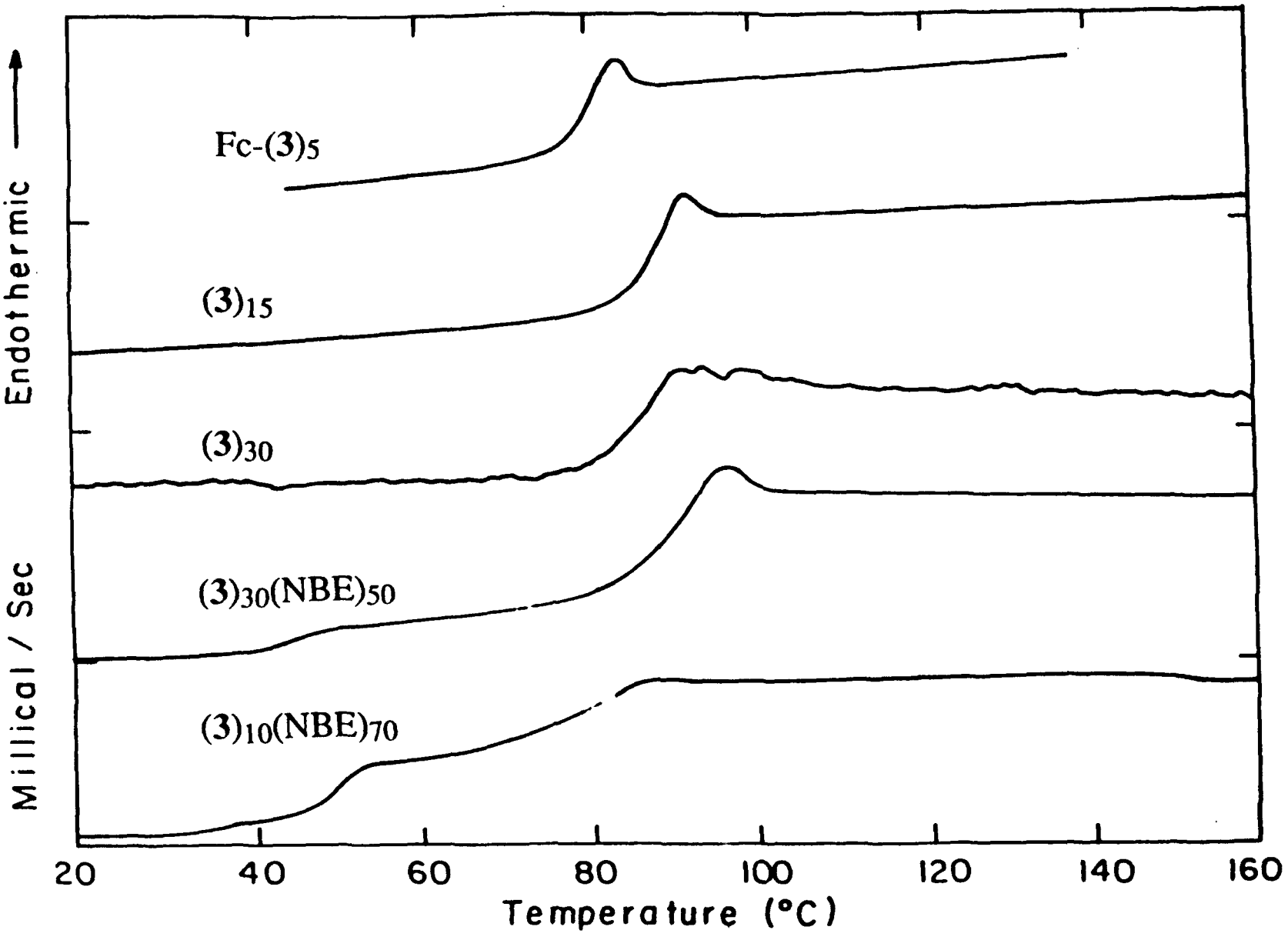
Endothermic
Millical / Sec
Fc-(3)5
(3)15
(3)30
(3)30(NBE)50
(3)10(NBE)70
20
40
60
80
100
120
140
160
Temperature (°C)

Fig. 6

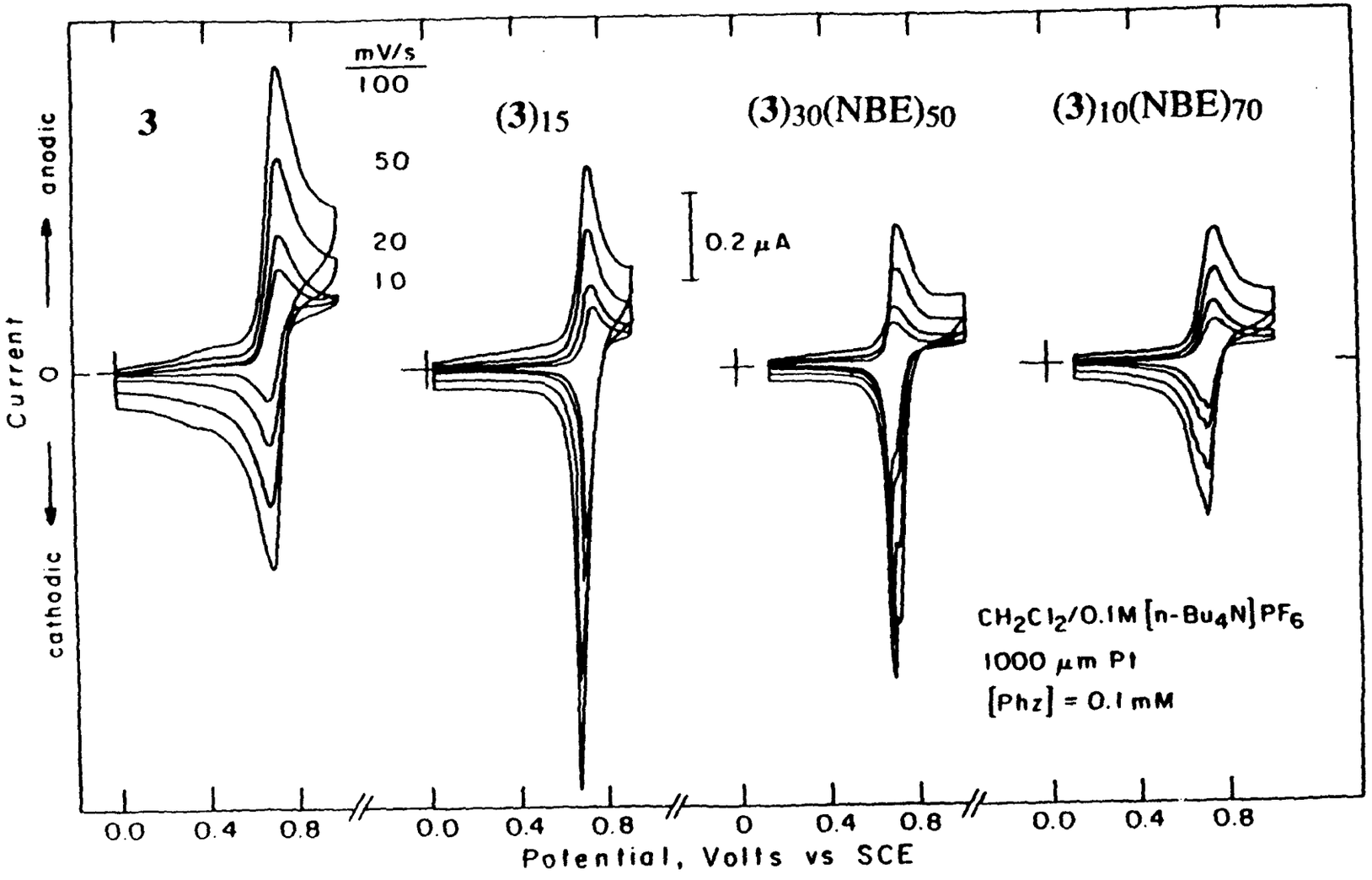
mV/s
100
50
20
10
3
(3)15
(3)30(NBE)50
(3)10(NBE)70
0.2 μA
Current
anodic
cathodic
0
CH2Cl2/0.1M [n-Bu4N]PF6
1000 μm Pt
[Phz] = 0.1 mM
0.0
0.4
0.8
Potential, Volts vs SCE

Fig 7

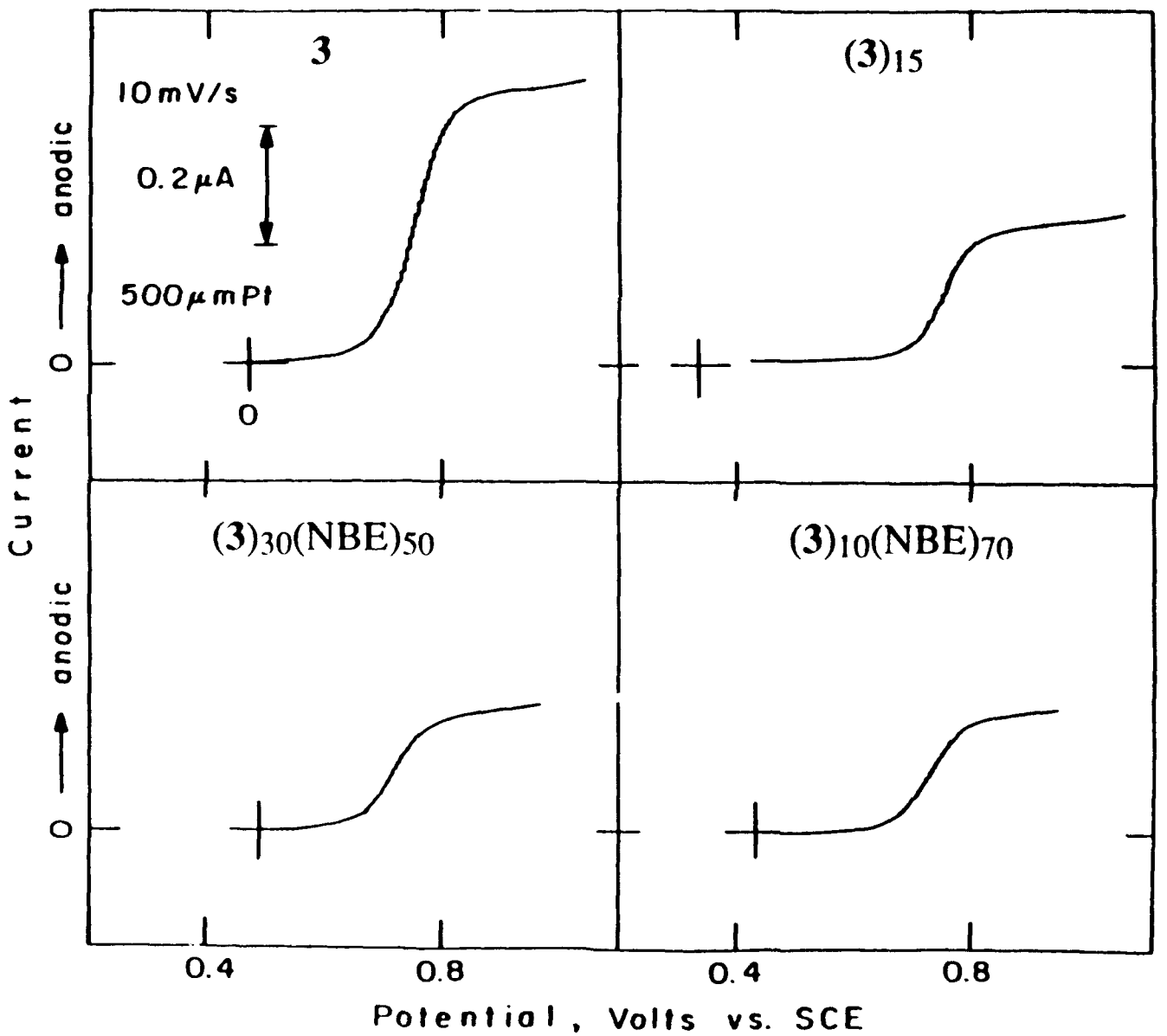
3
10 mV/s
0.2 μA
500 μm Pt
0
(3)15
(3)30(NBE)50
(3)10(NBE)70
Current
0 → anodic
0 → anodic
0.4
0.8
0.4
0.8
Potential, Volts vs. SCE

Fig 4

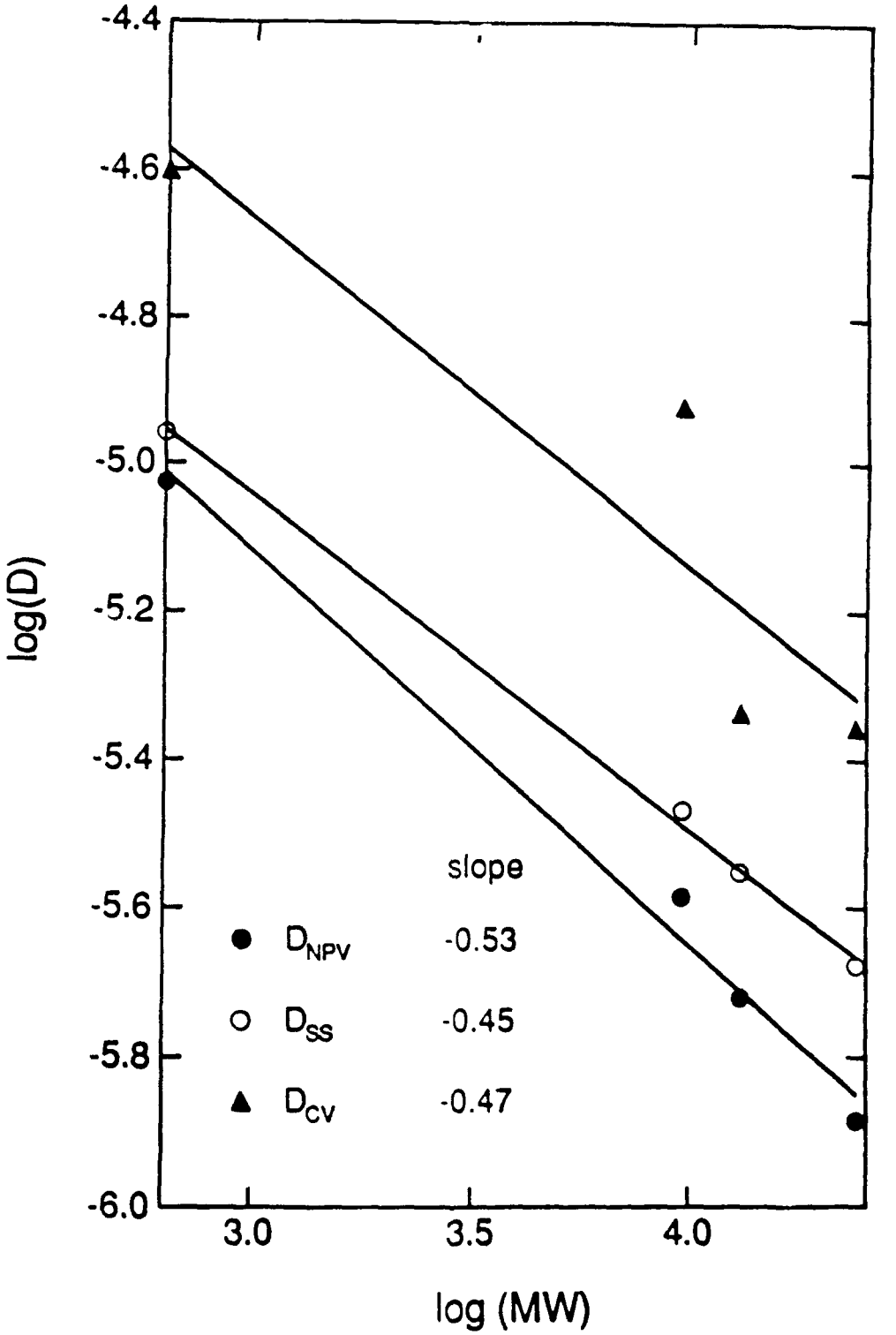
-4.4
-4.6
-4.8
-5.0
-5.2
-5.4
-5.6
-5.8
-6.0
log(D)
3.0
3.5
4.0
log (MW)
slope
D_{NPV} -0.53
D_{SS} -0.45
D_{CV} -0.47

Fig. 9

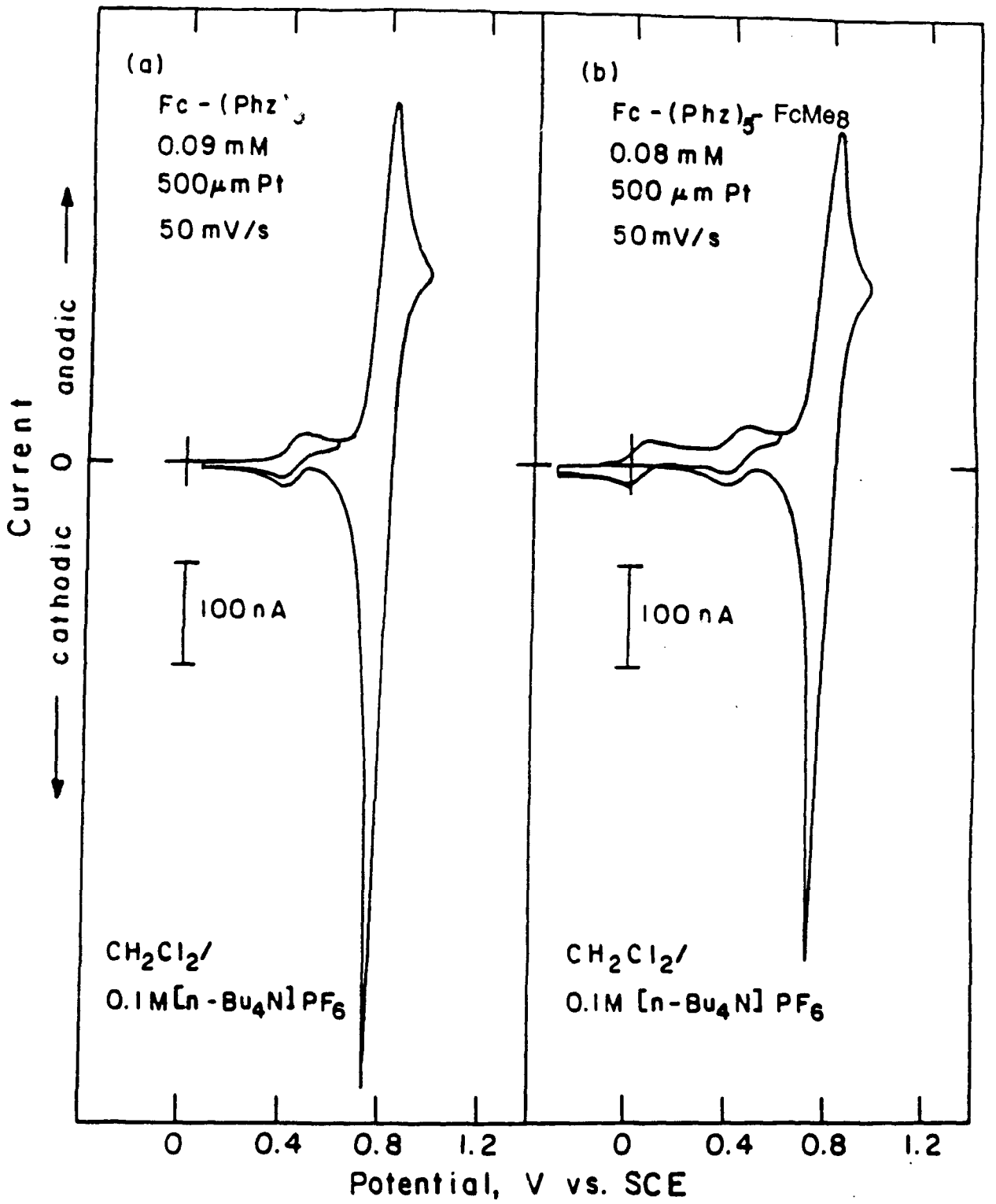
(a)
Fc - (Phz)3
0.09 mM
500μm Pt
50 mV/s
100 nA
CH2Cl2/
0.1M[n-Bu4N]PF6
(b)
Fc - (Phz)5 FcMe8
0.08 mM
500 μm Pt
50 mV/s
100 nA
CH2Cl2/
0.1M [n-Bu4N] PF6
Current
anodic
0
cathodic
0
0.4
0.8
1.2
Potential, V vs. SCE

Fig. 16

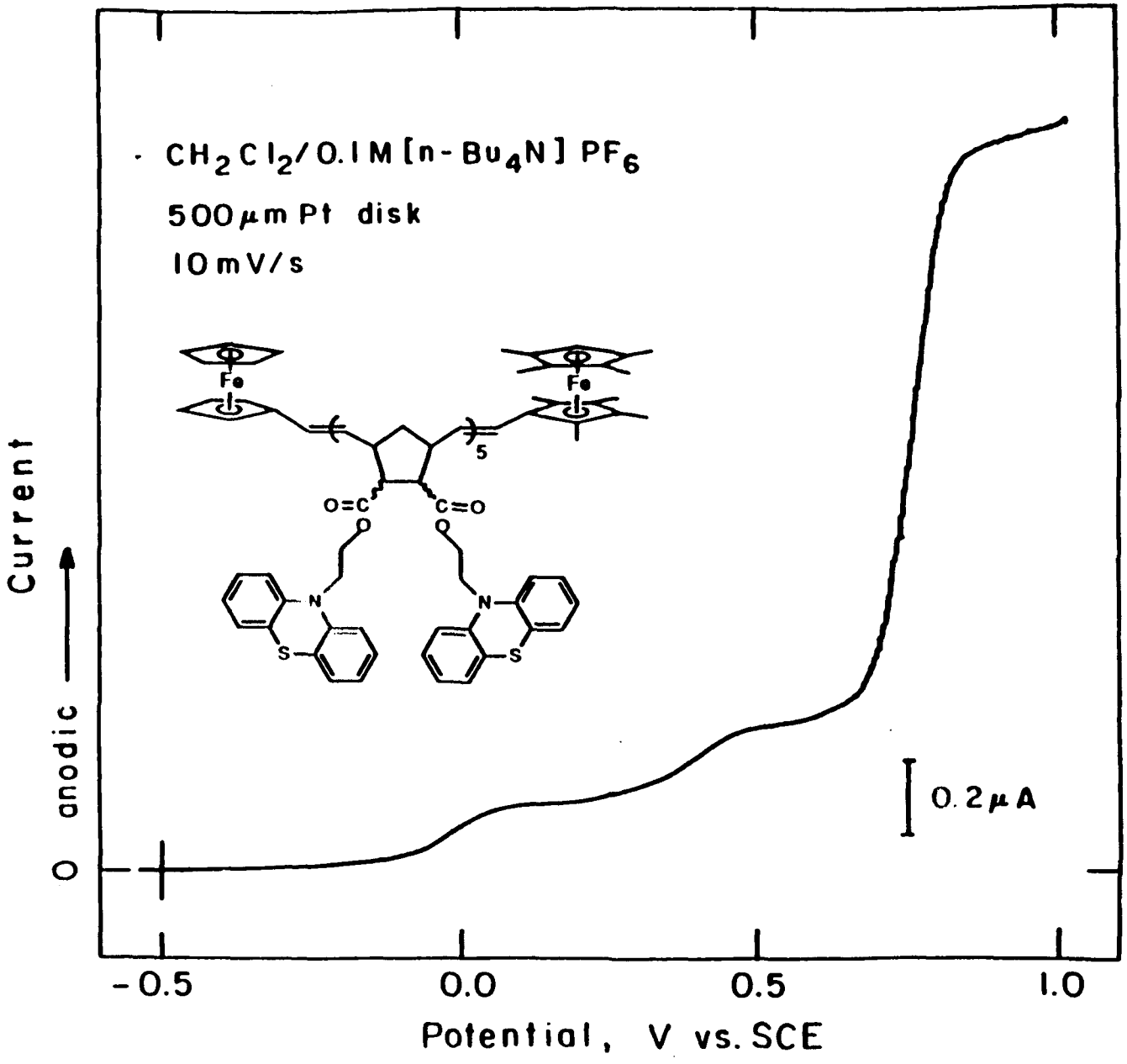
CH_2Cl_2/0.1M [n-Bu_4N] PF_6
500μm Pt disk
10mV/s
Fe
Fe
5
O=C
C=O
O
O
N
N
S
S
Current
0 anodic
0.2μA
-0.5
0.0
0.5
1.0
Potential, V vs. SCE

Fig 11

DL/1113/89/1

TECHNICAL REPORT DISTRIBUTION LIST, GENERAL

	No. Copies
Office of Naval Research Chemistry Division, Code 1113 800 North Quincy Street Arlington, VA 22217-5000	3
Commanding Officer Naval Weapons Support Center Attn: Dr. Bernard E. Douda Crane, IN 47522-5050	1
Dr. Richard W. Drisko Naval Civil Engineering Laboratory Code L52 Port Hueneme, California 93043	1
Defense Technical Information Center Building 5, Cameron Station Alexandria, Virginia 22314	2 high quality
David Taylor Research Center Dr. Eugene C. Fischer Annapolis, MD 21402-5067	1
Dr. James S. Murday Chemistry Division, Code 6100 Naval Research Laboratory Washington, D.C. 20375-5000	1
Dr. Ronald L. Atkins Chemistry Division (Code 385) Naval Weapons Center China Lake, CA 93555-6001	1
Chief of Naval Research Special Assistant for Marine Corps Matters Code 00MC 800 North Quincy Street Arlington, VA 22217-5000	1
Dr. Bernadette Eichinger Naval Ship Systems Engineering Station Code 053 Philadelphia Naval Base Philadelphia, PA 19112	1
Dr. Sachio Yamamoto Naval Ocean Systems Center Code 52 San Diego, CA 92152-5000	1
David Taylor Research Center Dr. Harold H. Singerman Annapolis, MD 21402-5067 ATTN: Code 283	1

30

15